

Sulphur ion implantation into O₂, CO, and CO₂ ices: Implications for the formation of sulphur-bearing molecules in the Kuiper Belt

Duncan V. Mifsud^{a,b,*}, Zuzana Kaňuchová^{c,**}, Péter Herczku^b, Zoltán Juhász^b,
Sándor T.S. Kovács^b, Gergő Lakatos^{b,d}, K.K. Rahul^b, Richárd Rác^b, Béla Sulik^b, Sándor Biri^b,
István Rajta^b, István Vajda^b, Sergio Ioppolo^{e,f}, Robert W. McCullough^g, Nigel J. Mason^{a,b,*}

^a Centre for Astrophysics and Planetary Science, School of Physics and Astronomy, University of Kent, Canterbury CT2 7NH, United Kingdom

^b Atomic and Molecular Physics Laboratory, HUN-REN Institute for Nuclear Research (Atomki), Debrecen H-4026, Hungary

^c Astronomical Institute, Slovak Academy of Sciences, Tatranská Lomnica SK-059 60, Slovakia

^d Institute of Chemistry, University of Debrecen, Debrecen H-4032, Hungary

^e Centre for Interstellar Catalysis, Department of Physics and Astronomy, Aarhus University, Aarhus DK-8000, Denmark

^f School of Electronic Engineering and Computer Science, Queen Mary University of London, London E1 4NS, United Kingdom

^g Department of Physics and Astronomy, School of Mathematics and Physics, Queen's University Belfast, Belfast BT7 1NN, United Kingdom

ARTICLE INFO

Keywords:

Sulphur

Ice

Kuiper Belt

Infrared spectroscopy

Astrochemistry

ABSTRACT

Previous experimental work has systematically investigated the radiolytic sulphur chemistry arising as a result of the implantation of reactive sulphur ions into various oxygen-bearing molecular ices (e.g., H₂O, CO₂) so as to better understand the surface chemistry of the Galilean moons of Jupiter, where sulphur ions are sourced from the giant Jovian magnetosphere. However, significantly less attention has been paid to analogous sulphur chemistry occurring under conditions relevant to the Kuiper Belt, where sulphur ions supplied by the solar wind may implant into the surfaces of icy bodies that are rich in volatile oxygen-bearing molecular ices such as O₂, CO, or CO₂. This paper presents the results of a study on the implantation of 290–400 keV S⁺ ions into pure O₂, CO, and CO₂ ices under temperature, pressure, radiation dose, and ice deposition conditions relevant to the Kuiper Belt, with a particular focus on the potential synthesis of simple inorganic sulphur-bearing molecules (e.g., SO₂, OCS, CS₂). Experiments involving CO₂ ices were also performed at higher temperatures more typically associated with the Galilean moon system so as to determine whether there exist any differences in the chemistry resulting from the implantation of reactive sulphur ions in these two regions of the Solar System. Our results constitute the first systematic investigation of solid-phase sulphur chemistry in the Kuiper Belt mediated by the sulphur ion component of the solar wind, and thus represent an important step forward in our understanding of the astrochemical processes occurring in the outermost depths of the Solar System.

1. Introduction

The implantation of reactive sulphur ions into astrophysical ice analogues at circa 80 K has been investigated in some detail by previous laboratory studies seeking to better comprehend the surface sulphur chemistry of the icy Galilean moons of Jupiter, where sulphur ions supplied by the giant Jovian magnetosphere continually bombard the surfaces of these moons (Mifsud et al., 2021a). These studies have demonstrated that the implantation of reactive sulphur ions constitutes

an important part of the so-called ‘radiolytic sulphur cycle’, wherein sulphur is cycled through various molecular forms as a result of its interaction with ionising radiation (Carlson et al., 1999; Carlson et al., 2002). In particular, it has been shown that the implantation of magnetospheric sulphur ions into the H₂O-rich surface ices of these moons results in the efficient synthesis of H₂SO₄ hydrates (Strazzulla et al., 2007; Strazzulla et al., 2009; Ding et al., 2013; Anders and Urbassek, 2019a; Anders and Urbassek, 2019b; Li and Li, 2023), which may then decompose to solid-phase SO₂ upon prolonged exposure to

* Corresponding authors at: Centre for Astrophysics and Planetary Science, School of Physics and Astronomy, University of Kent, Canterbury CT2 7NH, United Kingdom.

** Corresponding author.

E-mail addresses: mifsud.duncan@atomki.hu (D.V. Mifsud), zkanuch@ta3.sk (Z. Kaňuchová), n.j.mason@kent.ac.uk (N.J. Mason).

<https://doi.org/10.1016/j.icarus.2023.115926>

Received 14 May 2023; Received in revised form 11 December 2023; Accepted 16 December 2023

Available online 19 December 2023

0019-1035/© 2023 The Authors. Published by Elsevier Inc. This is an open access article under the CC BY-NC-ND license (<http://creativecommons.org/licenses/by-nc-nd/4.0/>).

ionising radiation (Hochanadel et al., 1955; Carlson et al., 2002; Loeffler et al., 2011). Indeed, these laboratory-deduced processes and mechanisms are consistent with the observed distributions of H₂SO₄ hydrates and SO₂ on Europa (Hendrix et al., 2011; Becker et al., 2022).

Although it is evident that significant efforts have been made to understand the radiation physics and chemistry induced as a result of the implantation of sulphur ions under conditions relevant to the icy Galilean moons of Jupiter, comparatively little headway has been made in understanding analogous processes in the context of the Kuiper Belt. In this region of the Solar System, sulphur ion delivery to icy objects is mediated by the solar wind (Giammanco et al., 2007); indeed, based on measurements of the solar wind S/O ratio at 1 AU by von Steiger et al. (2010), Ruf et al. (2019) were able to determine that a flux of 1.58 sulphur ions cm⁻² s⁻¹ is expected at 50 AU. Recent experiments by Ruf et al. (2019) and Ruf et al. (2021) highlighted the potential significance of solar wind-mediated sulphur ion implantations into the icy surfaces of Kuiper Belt Objects (KBOs) by demonstrating that the implantation of 105 keV S⁷⁺ ions into both molecular ice mixtures as well as non-sulphur-bearing organic residues representative of those on the surfaces of KBOs results in the formation of well over one thousand individual organosulphur molecules with molecular weights ranging up to 900 amu. These results are suggestive of an active and advanced sulphur chemistry in the coldest depths of the outer Solar System that is mediated by the sulphur ion component of the solar wind. Moreover, these results also complement the recently published detection of large and complex organosulphur molecules on the surface of comet 67P/Churyumov-Gerasimenko (Mahjoub et al., 2023).

The formation of novel sulphur-bearing molecules as a result of the implantation of reactive sulphur ions into astrophysical ice analogues relevant to the surfaces of KBOs was also considered by Lv et al. (2014), who studied the implantation of 176 keV S¹¹⁺ and 90 keV S⁹⁺ ions into CO and CO₂ ices, respectively. Their experiments, conducted at 15 K, revealed that both systems yielded SO₂ as a radiolysis product, and that OCS was also formed as a result of sulphur ion implantation into CO ice. Follow-up studies by Boduch et al. (2016) did not detect SO₂ after the implantation of 144 keV S⁹⁺ ions into pure CO₂ and O₂ ices at 16 K, nor after implantation into mixtures of these ices with H₂O, thereby contrasting with the previous results of Lv et al. (2014). It should be noted, however, that Boduch et al. (2016) made use of ultraviolet absorption spectroscopy as their product detection method, and so it is therefore possible that the formation of SO₂ was masked by the strong absorption features of O₃ or the sulphur oxyanions and radical anions that were detected after sulphur ion implantation into these ices. Indeed, SO₂ was later detected as a product of the implantation of 290 keV S⁺ ions into CO₂ ice at 20 K by Mifsud et al. (2022a), who relied on infrared absorption spectroscopy as their primary product detection method.

In this paper, we present the results of a systematic study on the implantation of 290–400 keV S⁺ ions into pure ices of O₂, CO, and CO₂ under temperature, pressure, radiation dose, and ice deposition conditions relevant to icy objects in the Kuiper Belt, with a particular focus on the possible formation of SO₂. Experiments made use of high projectile ion fluences ($F > 10^{16}$ ions cm⁻²) and were nominally carried out at 20 K, although the implantation of sulphur ions into CO₂ ice was also performed at 70 K so as to allow for a direct comparison between the sulphur radiation astrochemistry postulated to be taking place in the Kuiper Belt with that known to occur on the surfaces of the more thoroughly studied icy Galilean moons of Jupiter. Our experimental methodology is described in detail in Section 2, while our results and their implications for sulphur chemistry in the Kuiper Belt are discussed in Section 3. A summative conclusion is provided in Section 4.

2. Experimental methodology

Sulphur ion implantation experiments were performed using the Ice Chamber for Astrophysics-Astrochemistry (ICA); a laboratory astrochemistry chamber located at the HUN-REN Institute for Nuclear

Research (Atomki) in Debrecen, Hungary. This set-up (Fig. 1) has been described in great detail in previous publications (Herczku et al., 2021; Mifsud et al., 2021b), and so only the most salient details will be discussed in this paper. The ICA is an ultrahigh-vacuum compatible stainless-steel chamber that may be evacuated to base pressure levels of about 10⁻⁹ mbar by the combined action of a turbomolecular pump and a dry rough vacuum pump. The chamber hosts a gold-coated oxygen-free high-conductivity copper sample holder at its centre, into which up to four infrared-transparent ZnSe deposition substrates may be mounted. The sample holder and the deposition substrates may be cooled to 20 K by means of a closed-cycle helium cryostat, although the working temperature may be set between 20 and 300 K by establishing a thermal equilibrium between the cooling effect of the cryostat and an internal cartridge heater.

Pure ices were prepared on the deposition substrates by means of background deposition of the respective gases (gas purities: O₂ = 99.995%, CO = 99.97%, CO₂ = 99.995%; all sourced from Linde) at a chamber pressure of a few 10⁻⁶ mbar. The deposition of the ices was monitored in situ using Fourier-transform mid-infrared transmission absorption spectroscopy over a spectral range of 4000–650 cm⁻¹ and at a spectral resolution of 1 cm⁻¹. The column density N (molecules cm⁻²) and thickness d (μm) of a deposited ice sample were quantified through the acquired mid-infrared spectra by employing Eqs. 1 and 2:

$$N = 2.303 \times \frac{P}{A_{\nu}} \quad (1)$$

$$d = 10,000 \times \frac{Nm}{\rho N_A} \quad (2)$$

where P is the area of a characteristic mid-infrared absorption band of the ice species (cm⁻¹), A_{ν} is the integrated band strength constant associated with that band (cm molecule⁻¹), m is the molecular weight of the molecule (g mol⁻¹), ρ is the density of the ice (g cm⁻³), and N_A is the Avogadro constant. Note that the constant 2.303 in Eq. (1) allows for the relation of P (which is measured from spectra on an absorbance scale) to A_{ν} (which is measured on an optical depth scale), while the constant 10,000 in Eq. (2) allows for d to be expressed in units of μm. A list of the ice densities and mid-infrared band strength constants that were used in this study is provided in Table 1.

The most prominent mid-infrared absorption bands in the spectra of solid CO and CO₂ are those respectively attributed to the stretching and asymmetric stretching modes at 2139 and 2343 cm⁻¹ (Isokoski et al., 2013; Smith et al., 2021). However, these absorption bands saturate fairly quickly during ice deposition; indeed, saturation occurs before the ices reach a suitable thickness for ion implantation to be carried out. Therefore, the less intense absorption bands related to the ¹³CO stretching and ¹³CO₂ asymmetric stretching modes respectively located at 2092 and 2282 cm⁻¹ were instead used to quantify the column densities and thicknesses of the deposited ices. To do this, a mid-infrared spectrum of the ice was acquired just prior to the saturation of the intense ¹²CO or ¹²CO₂ bands and the ¹²C:¹³C column density ratio was measured for each molecule. Continued deposition then resulted in the saturation of the intense ¹²CO or ¹²CO₂ bands, after which the measured ¹³CO or ¹³CO₂ column densities were used in combination with the experimental isotopologue abundance ratio to determine the total molecular column densities of the deposited ices and their thicknesses. A similar approach was previously used by Lv et al. (2014) and Mifsud et al. (2022a).

A challenge exists in quantifying the column density and thickness of a deposited O₂ ice, due to the fact that this species is a homonuclear diatomic molecule and is thus infrared-inactive. Given the similar molecular geometries, molecular weights, and chamber pumping speeds of the CO and O₂ molecules, we have assumed that depositing a O₂ ice at the same chamber pressure and for the same duration as was done for the CO ice would result in a similar column density being deposited.

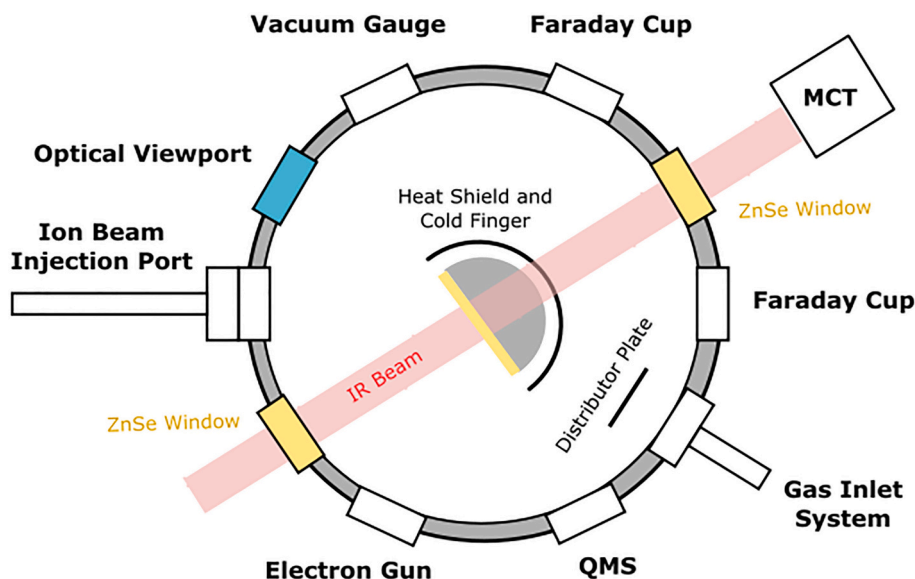


Fig. 1. Top-view schematic diagram of the ICA set-up. Ion irradiation and implantation experiments are performed using the depicted arrangement, with projectile ions impacting the surfaces of the deposited ices at an angle of 36° to the normal and the infrared spectroscopic beam being maintained orthogonal to the ices. Image reproduced from Mifsud et al. (2021b) with the kind permission of the European Physical Journal.

Table 1

A list of the mid-infrared band positions, their associated integrated band strength constants, and ice densities used in this study.

Molecule	Mid-Infrared Band Position (cm^{-1})	A_v ($10^{-17} \text{ cm molecule}^{-1}$)	ρ (g cm^{-3})	References
SO ₂	1343 (ν_3)	1.47	–	Garozzo et al. (2008)
O ₂	–	–	1.53	Freiman and Jodl (2004)
CO	2139 ($^{12}\text{CO } \nu_3$)	1.10	0.88	Gerakines et al. (1995), Luna et al. (2022)
	2092 ($^{13}\text{CO } \nu_3$)	1.30		
CO ₂	2343 ($^{12}\text{CO}_2 \nu_3$)	7.60	0.98 (20K)	Gerakines et al. (1995), Satorre et al. (2008)
	2282 ($^{13}\text{CO}_2 \nu_3$)	7.80	1.48 (70 K)	

Given that the density of solid O₂ is known (Table 1), the thickness could then be easily calculated.

All target ices were deposited to an initial thickness of about $3 \mu\text{m}$, which is greater than the penetration depths of the projectile sulphur ions used in this study ($<1.2 \mu\text{m}$; Ziegler et al., 2010), thus ensuring the implantation of the ions within the ice. Once the ice was deposited to this thickness, a pre-irradiation mid-infrared spectrum of the ice was acquired after which it was exposed to a sulphur ion beam delivered by a Tandatron particle accelerator (Rajta et al., 2018; Biri et al., 2021) connected directly to the ICA (Fig. 1), with typical ion beam fluxes of $2.76 \times 10^{11} \text{ ions cm}^{-2} \text{ s}^{-1}$ being used. Additional spectra were collected at various ion fluence intervals during irradiation until a total fluence of $>10^{16} \text{ ions cm}^{-2}$ was implanted. Given that the expected sulphur ion flux at 50 AU is $1.58 \text{ ions cm}^{-2} \text{ s}^{-1}$ (von Steiger et al., 2010; Ruf et al., 2019), the fluences delivered in our experiments correspond to 200 million years of solar wind-mediated sulphur ion delivery to icy KBOs. A summary of the experiments carried out in this study is given in Table 2.

During the experiments, it was noted that sulphur ion implantation resulted in sputtering leading to a gradual thinning of the ice. To compensate for this loss of target material, a simultaneous deposition-irradiation method was used. In this method, after initial deposition of the target ice to a thickness of $3 \mu\text{m}$, the ices were irradiated by the sulphur ion beam with concurrent background deposition of more ice at

Table 2

Summary of the sulphur ion implantation experiments performed in this study.

Experiment	Target Ice	Temperature (K)	S ⁺ Ion Energy (keV)	Implantation Depth (μm)	Fluence Delivered ($10^{16} \text{ ions cm}^{-2}$)
1	O ₂	20	400	0.62	1.01
2	CO	20	400	1.13	1.11
3	CO ₂	20	290	0.66	1.01
4	CO ₂	70	290	0.44	1.25

a chamber pressure of about 10^{-5} mbar , with both irradiation and deposition being halted during mid-infrared spectral acquisition. The possibility of the ion beam interacting with gas-phase O₂, CO, and CO₂ resulting in molecular dissociation and the subsequent incorporation of the resultant fragments and radicals into the depositing ice is not anticipated to impact the chemical evolution of the ice in any significant way (see the work of Mifsud et al. (2022a) for further evidence supporting this claim).

However, it should be acknowledged that the use of a simultaneous deposition-irradiation method may result in the better trapping of radiolytically generated volatiles when compared to other methodologies in which fresh overlayers of ice are not continuously deposited (Teolis et al., 2005; Teolis et al., 2006). This should not be viewed as a disadvantage, as the trapping of such volatiles allows for their accumulation within the ice and their participation in the various chemical reaction networks present there, thus further contributing to the chemical diversity and abundance of products formed. Moreover, the continuous deposition of fresh ice layers better mimics the ongoing condensation of molecular material on the surfaces of outer Solar System bodies due to the effect of gravity or the re-deposition of material previously ejected from the surface as a result of micrometeorite impact, cryovolcanism, sublimation, or ion-induced sputtering. In this regard, the methodology used in this present study differs to those used in previous experiments on the implantation of reactive sulphur ions into astrophysical ice analogues, where single deposition (i.e., where the initially deposited ice was not replenished at any point during the experiment) or sequential deposition-irradiation methodologies were used instead (Ding et al., 2013; Lv et al., 2014; Boduch et al., 2016).

3. Results and discussion

3.1. 400 keV S⁺ ion implantation into O₂ ice at 20 K

The implantation of reactive sulphur ions into pure O₂ ice represents perhaps the simplest chemical route towards the formation of SO₂. Such a process is therefore directly relevant to comets in whose icy nuclei O₂ is a relatively abundant molecule (Luspay-Kuti et al., 2018), including those of Kuiper Belt origin such as 67P/Churyumov-Gerasimenko (Bieler et al., 2015; Mousis et al., 2016) as well as those of Oort Cloud origin such as 1P/Halley (Rubin et al., 2015). Despite this, the laboratory study of reactive sulphur ion implantation into solid O₂ has thus far only been performed using ultraviolet absorption spectroscopy (Boduch et al., 2016). Although certainly a useful analytical technique, this region of the electromagnetic spectrum is not ideally suited for molecular identification. As such, the results described in this present section constitute the first investigation of sulphur ion implantation into a low-temperature O₂ ice using mid-infrared absorption spectroscopy, thus allowing for the more secure identification of radiolytic product species.

The implantation of 400 keV S⁺ ions into solid O₂ at 20 K results in the formation of new mid-infrared absorption bands (Fig. 2). The most prominent of these bands is that at about 1040 cm⁻¹ attributable to the formation of O₃ (Chaabouni et al., 2000). Indeed, the synthesis of O₃ as a result of the irradiative processing of O₂ ice has been studied thoroughly (e.g., Famá et al., 2002; Bennett and Kaiser, 2005; Sivaraman et al., 2007; Ennis et al., 2011), and therefore will be discussed only very briefly in this paper. The radiolytic synthesis of O₃ proceeds via a two-step reaction sequence first involving the homolytic molecular dissociation of O₂ to supra-thermal oxygen atoms followed by the addition of one such atom to O₂. Such an addition reaction has been considered to be either energetically barrierless (Bennett and Kaiser, 2005; Sivaraman et al., 2007), or else as having a small activation energy barrier of <0.5 eV (Ioppolo et al., 2008).

Of particular interest is the appearance of two distinct absorption features at about 1343 and 1150 cm⁻¹ that appear after an ion fluence of about 2.5 × 10¹⁵ S⁺ ions cm⁻² is supplied to the ice and which continue to grow during sulphur ion implantation until a fluence of 9 × 10¹⁵ S⁺ ions cm⁻², after which the areas of these bands plateau (Figs. 2 and 3). It

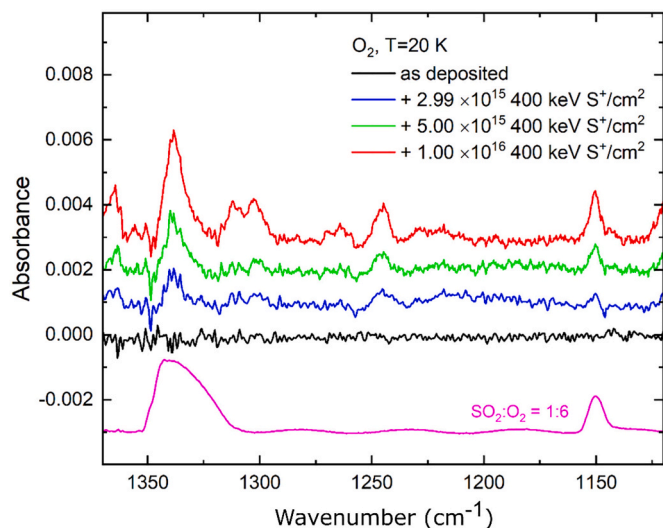


Fig. 2. Mid-infrared spectra of solid O₂ before (black trace) and during (blue, green, and red traces) the implantation of 400 keV S⁺ ions at 20 K. Also shown is the mid-infrared spectrum of an unirradiated SO₂:O₂ (1:6) ice mixture at 20 K (pink trace). Note that the spectra were acquired using background spectra of the bare ZnSe substrates at 20 K. Note also that spectra are vertically shifted for clarity. (For interpretation of the references to colour in this figure legend, the reader is referred to the web version of this article.)

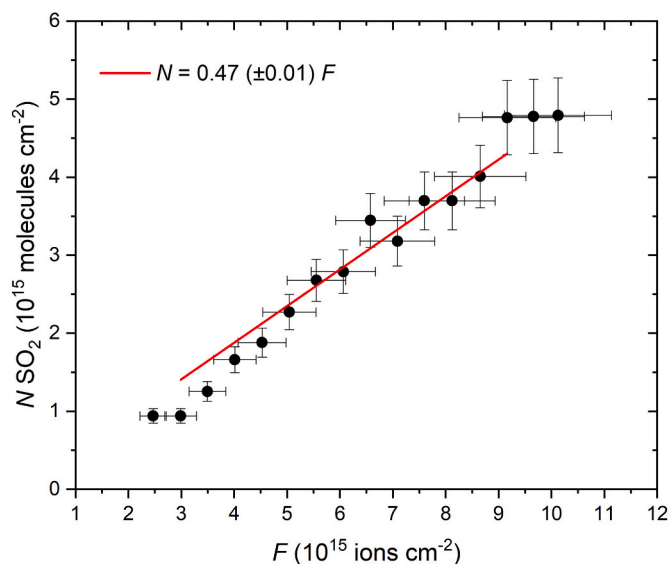


Fig. 3. Evolution of measured SO₂ column density during the implantation of 400 keV S⁺ ions into solid O₂ at 20 K. The linear fit indicated by the red line has been applied over the fluence interval (3.5–9.2) × 10¹⁵ S⁺ ions cm⁻². (For interpretation of the references to colour in this figure legend, the reader is referred to the web version of this article.)

is worth noting that the intensity of the absorption band at 1343 cm⁻¹ is consistently greater than that of the band at 1150 cm⁻¹ throughout the ion implantation process. The positions and relative intensities of these bands are therefore in good agreement with the asymmetric and symmetric stretching modes of SO₂ (Schriver-Mazzuoli et al., 2003; Mifsud et al., 2023) and, indeed, a comparison with a control spectrum of an unirradiated SO₂:O₂ (1:6) mixed ice prepared by depositing a pre-mixed gas mixture at 20 K demonstrated a remarkably good degree of similarity (Fig. 2). As such, the bands that appear at 1343 and 1150 cm⁻¹ can be attributed to the formation of SO₂.

Fig. 3 depicts the evolution of the column density of SO₂ during the implantation of 400 keV S⁺ ions into O₂ ice at 20 K as a function of fluence. These column densities were calculated by measuring the band area of the asymmetric stretching mode at 1343 cm⁻¹ and making use of an integrated band strength constant of 1.47 × 10⁻¹⁷ cm molecule⁻¹ (Garozzo et al., 2008, Table 1). It is possible to note that the initial increase in SO₂ column density is negligible up to a fluence of about 3 × 10¹⁵ S⁺ ions cm⁻², after which it begins to increase in a linear fashion until a fluence of 9 × 10¹⁵ S⁺ ions cm⁻² is reached. Beyond this fluence, however, the SO₂ abundance remains fairly constant. By applying a zero-intercept trendline through the linear portion of the data presented in Fig. 3 (corresponding to fluences between (3.0–9.2) × 10¹⁵ S⁺ ions cm⁻²), we have been able to deduce that the SO₂ formation rate in this fluence regime is 0.47 (±0.01) SO₂ molecules per impinging 400 keV S⁺ ion, which compares fairly well with the formation rate of 0.38 (±0.20) SO₂ molecules per impinging 90 keV S⁹⁺ ion into CO₂ ice as reported by Lv et al. (2014).

The observed formation of SO₂ after the implantation of 400 keV S⁺ ions into O₂ ice at 20 K contrasts with the results of Boduch et al. (2016), who studied the implantation of 144 keV S⁹⁺ ions into solid O₂ at 16 K using ultraviolet absorption spectroscopy but did not detect the formation of SO₂. Instead, the main sulphurous product reported by those authors was the SO₃⁻ radical anion which presents a strong and board absorption band centred at approximately 255 nm (Dogliotti and Hayon, 1968; Waygood and McElroy, 1992). This band may have possibly obscured any ultraviolet absorption bands attributable to SO₂, such as that expected at 276 nm (Holtom et al., 2006; Mason et al., 2006). Nevertheless, the results of this present study clearly demonstrate that sulphur ion implantation into O₂ ice at cold (i.e., 15–20 K) temperatures

does indeed result in the formation of SO₂.

This apparently favourable method for SO₂ synthesis has interesting implications for sulphur chemistry on cometary bodies. Indeed, SO₂ represents the third most abundant sulphur-bearing species (after H₂S and atomic sulphur) in both the bulk ices and coma of comet 67P/Churyumov-Gerasimenko (Calmonte et al., 2016; Rubin et al., 2019). Analysis of the O₂ content of 67P/Churyumov-Gerasimenko and 1P/Halley has led to the suggestion that O₂ may be a relatively abundant component of comets originating in the outermost reaches of the Solar System, with respective abundances of $3.80 \pm 0.85\%$ and $3.7 \pm 1.7\%$ relative to H₂O having been measured (Bieler et al., 2015; Rubin et al., 2015). Strong arguments have been put forward in favour of a primordial pre-solar origin of this O₂ (Mousis et al., 2016), wherein the radiolytic processing of H₂O-rich interstellar icy grain mantles by galactic cosmic rays produces O₂ (Grievies and Orlando, 2005; Zheng et al., 2006a; Zheng et al., 2006b; Zheng et al., 2007; Mifsud et al., 2022b) which is then stabilised in the solid phase as clathrate hydrates (Mayer and Hallbrucker, 1989; Hallbrucker and Mayer, 1990). It is from these interstellar icy grain mantles that cometary bodies such as 67P/Churyumov-Gerasimenko and 1P/Halley are ultimately formed (Rubin et al., 2015; Mousis et al., 2016).

Therefore, if sulphur ion implantation into the (relatively) abundant O₂ ices is to be proposed as a potential contributor to the synthesis of SO₂ in comets then physical and chemical processes associated with the radiolytic processing of the H₂O molecules associated with the clathrate hydrate must also be taken into account. This processing likely contributes to some extent to the ejection of molecular material via sputtering (Baragiola, 2003), but also produces a plethora of hydrogen atoms and OH radicals as a result of the dissociation of the H₂O molecules. These reactive radical species may suppress the formation of O₃ (the major product of the radiolytic processing of O₂) by engendering its dissociation to O₂ and OH (Lee et al., 1978; Ioppolo et al., 2008; Mokrane et al., 2009). This is in agreement with the hitherto non-detection of O₃ in the bulk ices or coma of 67P/Churyumov-Gerasimenko or any other comet (Altwegg, 2018). The suppression of O₃ formation in an icy environment also characterised by the presence of H₂O and SO₂ is actually advantageous from the perspective of preserving the SO₂ content of the ice, as O₃ is known to oxidise SO₂ to HSO₄⁻ anions when in the presence of H₂O (Erickson et al., 1977; Penkett et al., 1979; Loeffler and Hudson, 2016).

Nevertheless, the formation of SO₂ in cometary ices as a result of sulphur ion implantation into O₂ ices is likely to be offset by other competing chemical processes. The first of these is the synthesis of H₂SO₄ hydrates: it is to be recalled that the implantation of sulphur ions into H₂O ices results in the efficient synthesis of these acid hydrates (Strazzulla et al., 2007; Strazzulla et al., 2009; Ding et al., 2013), and thus it is possible that a sulphur ion that is implanted in the cometary O₂ clathrate hydrate interacts with a H₂O molecule rather than a O₂ molecule thereby reducing the formation efficiency of SO₂. Moreover, if the comet experiences any increases in temperature, then this would promote thermal reactions between H₂O and SO₂ molecules to yield the sulphur oxyanions HSO₃⁻ and S₂O₅²⁻ (Loeffler and Hudson, 2010; Loeffler and Hudson, 2016; Bang et al., 2017; Kaňuchová et al., 2017; Mifsud et al., 2021b). Similar depletions in the SO₂ content of the comet would be expected if it suddenly experienced a significantly higher radiation dose, as the irradiation of ice mixtures containing H₂O and SO₂ has been shown to also yield H₂SO₄ hydrates and sulphur oxyanions (Moore et al., 2007). Such changes in the temperature and radiation dose experienced by the comet may occur, for example, when it is first ejected from the Kuiper Belt and set into a highly eccentric elliptical orbit around the sun.

To summarise, we have, for the first time, conclusively demonstrated that the implantation of reactive sulphur ions into O₂ ices under experimental conditions representative of those found in the Kuiper Belt yields SO₂ at a calculated efficiency of 0.47 (±0.01) SO₂ molecules per impinging 400 keV S⁺ ion. This sets an upper limit to the SO₂ molecules formed in this fashion on an icy KBO (e.g., a comet) over the course of

the existence of the Solar System of approximately 10¹⁷ molecules cm⁻² (assuming there has been no significant variation in the sulphur ion flux at 50 AU during this time). The efficiency of this SO₂ formation mechanism is, however, likely hindered by competing reactions (e.g., the interaction of implanted sulphur ions with cometary H₂O molecules to yield H₂SO₄ hydrates), and thermal and radiation chemistry could further decrease the abundance of SO₂ after its formation. Although it is still likely that the majority of cometary SO₂ was accrued during the formation of the comet in pre-solar environments such as dense interstellar clouds, our present results demonstrate that sulphur ion implantation from the solar wind into O₂-bearing KBOs may represent a non-negligible route towards SO₂ synthesis.

3.2. 400 keV S⁺ ion implantation into CO ice at 20 K

The implantation of 400 keV S⁺ ions into solid CO at 20 K resulted in the appearance of several new mid-infrared absorption bands, many of which were clustered in the 2400–2200 cm⁻¹ wavenumber range associated with the C=O bond stretching modes of various molecules (Fig. 4). Based on previous assignments by a number of studies (e.g., Strazzulla et al., 1997; Gerakines and Moore, 2001; Trotter and Brooks, 2004; Loeffler et al., 2005; Palumbo et al., 2008; Lv et al., 2014), it has been possible to assign these bands to molecules belonging to the cumulene dioxide family (of the type C_xO₂ where x > 2), oxocarbon molecular radicals (of the type C_xO where x > 1), as well as CO₂ and CO₃ (Table 3). It is presumed that the radiation chemistry leading to the formation of these species begins with the homolytic dissociation of the CO molecule to yield free supra-thermal carbon and oxygen atoms. Free carbon atoms may then subsequently react with surviving CO molecules to begin a catenation reaction sequence yielding sequentially larger oxocarbon molecular radicals. The growth of these radicals by sequential carbon addition may be quenched via the addition of a free oxygen atom at the radical terminus, which results in the formation of a closed-shell unsaturated cumulene dioxide species.

It is important to realise, however, that the formation of cumulene dioxides and oxocarbon radicals via the mechanistic chemistry described above requires a greater supply of carbon atoms sourced from CO dissociation than of oxygen atoms. As such, additional processes must exist which consume the remaining free oxygen atoms. Among

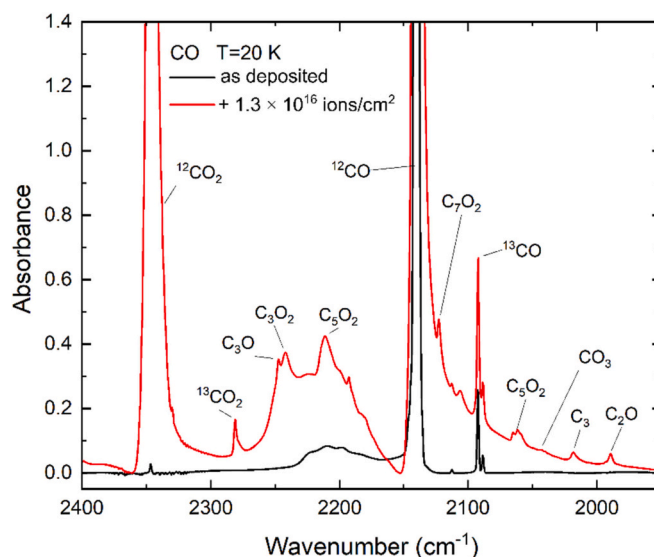


Fig. 4. Mid-infrared spectra of solid CO before (black trace) and after (red trace) the implantation of 400 keV S⁺ ions at 20 K. Note that spectra were acquired using background spectra of the bare ZnSe substrates at 20 K. (For interpretation of the references to colour in this figure legend, the reader is referred to the web version of this article.)

Table 3

List of oxocarbon molecules present in the CO ice irradiated by 400 keV S^{1+} ions sorted by the wavenumber position of their mid-infrared absorption bands. Band assignments are largely based on the previous works of [Trottier and Brooks \(2004\)](#), [Palumbo et al. \(2008\)](#), and [Lv et al. \(2014\)](#).

Molecule		Mid-Infrared Band Position (cm^{-1})
Formula	Name	
$^{12}\text{CO}_2$	Carbon dioxide	2343
$^{13}\text{CO}_2$	Carbon dioxide	2282
C_3O	Tricarbon monoxide	2247
C_3O_2	Tricarbon dioxide (carbon suboxide)	2242
C_5O_2	Pentacarbon dioxide	2221
^{12}CO	Carbon monoxide	2139
C_7O_2	Heptacarbon dioxide	2122
^{13}CO	Carbon monoxide	2092
C_5O_2	Pentacarbon dioxide	2059
CO_3	Carbon trioxide	2044
C_3	Catena-tricarbon	2019
C_2O	Dicarbon monoxide	1990

these processes is the formation of CO_2 as a result of the addition of a supra-thermal oxygen atom to CO; a process which has been described at some length in the literature ([Loeffler et al., 2005](#); [de Barros et al., 2011](#)). The addition of oxygen atoms to any nascent CO_2 results in the synthesis of CO_3 ([Sivaraman et al., 2013](#)); a minor quantity of which was observed in the mid-infrared spectrum of the processed CO ice ([Fig. 4](#)). Lastly, the formation of O_3 , noted by the appearance of its asymmetric stretching mode at about 1040 cm^{-1} ([Chaabouni et al., 2000](#)), could also act as a sink for free oxygen atoms in this experiment ([Fig. 5](#)).

A closer examination of the data shown in [Fig. 5](#) reveals that a small absorption feature is present at about 1345 cm^{-1} , and it is also possible that a very weak band is beginning to emerge against the sinusoidal background (this sinusoidal pattern is likely the result of interference caused as a result of changes to the thickness of the ice) at about 1150 cm^{-1} . The positions of these bands respectively coincide well with those of the asymmetric and symmetric stretching modes of solid SO_2 diluted in CO, as confirmed by a control experiment in which a mid-infrared

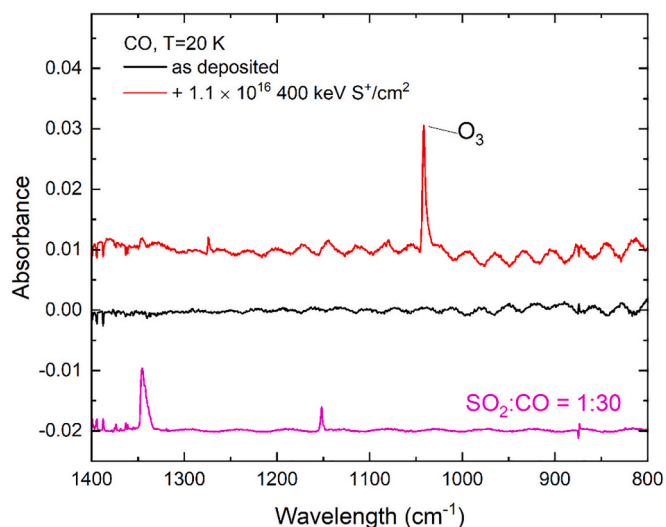


Fig. 5. Mid-infrared spectra of solid CO before (black trace) and after (red trace) the implantation of 400 keV S^{1+} ions at 20 K. Also shown is the mid-infrared spectrum of an unirradiated $\text{SO}_2:\text{CO}$ (1:30) ice mixture at 20 K (pink trace). Note that the spectrum of the irradiated ice is a difference spectrum yielded after the subtraction of the ‘as deposited’ spectrum. Note also that spectra are vertically shifted for clarity. (For interpretation of the references to colour in this figure legend, the reader is referred to the web version of this article.)

absorption spectrum of an unirradiated $\text{SO}_2:\text{CO}$ (1:30) ice prepared by depositing a pre-mixed gas mixture at 20 K was acquired ([Fig. 5](#)). It is therefore possible to state that SO_2 may have been formed in our CO ice as a result of sulphur ion implantation, but that the abundance present after implanting 10^{16} sulphur ions cm^{-2} was too small for the corresponding asymmetric and symmetric stretching modes to be unequivocally apparent against the background continuum and so any detection of SO_2 must be regarded as highly tentative at best.

It should be noted, however, that the positions of these supposed SO_2 bands in our irradiated CO ice match very well with those reported by [Lv et al. \(2014\)](#), who detected SO_2 formation after the implantation of 176 keV S^{11+} ions into CO ice at 15 K. In their study, [Lv et al. \(2014\)](#) found that the asymmetric and symmetric stretching modes of SO_2 only became evident against the background continuum in acquired difference spectra after a fluence of 1.9×10^{16} ions cm^{-2} had been delivered to the target ice, and quantified the formation efficiency of this molecule as being $0.20 (\pm 0.05)$ SO_2 molecules per impinging 176 keV S^{11+} ion. The fact that [Lv et al. \(2014\)](#) were only able to clearly discern the formation of SO_2 in their sulphur ion implantation experiments at a fluence that was nearly twice that delivered in this present study would seemingly reinforce our tentative detection of SO_2 . However, in the absence of any other confirmatory experiments (e.g., temperature-programmed desorption experiments of the irradiated ice in which the composition of the ice is monitored via mid-infrared spectroscopy and that of the gas phase is monitored via mass spectrometry), the detection of SO_2 as a result of the implantation of 400 keV S^{1+} ions into CO ice at 20 K as described in this study must remain tentative.

The sulphur chemistry initiated as a result of the implantation of reactive sulphur ions into CO ice at low temperature has important implications for icy KBOs. The presence of CO on the surface of a number of such KBOs has been reported, including the dwarf planet Pluto ([Cruikshank et al., 2015](#); [Grundy et al., 2016](#)), Neptune’s largest moon Triton ([Grundy et al., 2010](#)), and a number of inner Solar System comets thought to have originated in the Kuiper Belt such as 17P/Holmes and 29P/Schwassman-Wachmann ([Kossacki and Szutowicz, 2010](#); [Kossacki and Szutowicz, 2013](#)). These CO-rich bodies would thus have been exposed to sulphur ions supplied by the solar wind for long periods in their histories, therefore making it possible that the implantation of these ions into the surface ices would have resulted in the synthesis of, for example, SO_2 .

Indeed, if it were to be assumed that the SO_2 formation efficiency calculated by [Lv et al. \(2014\)](#) for the implantation of 176 keV S^{11+} ions into CO ice at 15 K is valid for the analogous synthesis at 20 K using 400 keV S^{1+} ions, then an estimation of the SO_2 formed on icy KBOs as a result of such an implantation process of about 4.5×10^{16} molecules cm^{-2} may be proposed. It is entirely possible, however, that the SO_2 formation efficiency as a result of the implantation of 176 keV S^{11+} ions into CO ice as estimated by [Lv et al. \(2014\)](#) is lower than that for the analogous process using 400 keV S^{1+} ions, as previous work on the implantation of sulphur ions into H_2O ice by [Ding et al. \(2013\)](#) has demonstrated that, although the ion charge state of the implanted sulphur ion bears no influence on the yield of sulphur-bearing products formed, more products were synthesised when higher energy ions were used as a projectile. Further study in this regard, including the use of projectile sulphur ions of different energies and higher ion fluences, is merited.

3.3. 290 keV S^{1+} ion implantation into CO_2 ice at 20 and 70 K

Experiments on the implantation of reactive sulphur ions into CO_2 ice at low temperatures (i.e., 20 K) have been previously performed by [Lv et al. \(2014\)](#) and [Boduch et al. \(2016\)](#) in an effort to understand the radiolytic sulphur cycle on Europa, where CO_2 ice exists as a minor component of the solid surface having an abundance of 0.036% by number relative to H_2O ([McCord et al., 1998](#); [Hand et al., 2007](#); [Hansen and McCord, 2008](#)) and where keV-MeV sulphur ions supplied by the giant Jovian magnetosphere continually bombard the surface at fluxes

of up to 10^8 ions $\text{cm}^{-2} \text{s}^{-1}$ (Dalton et al., 2013). However, the low temperatures at which these experiments were conducted make them arguably more relevant to CO_2 -rich icy bodies in the Kuiper Belt than to Europa (Ashkenazy, 2019; Ahrens et al., 2022; Brown and Fraser, 2023). By performing our experiments at both 20 and 70 K, we have been able to gauge whether temperature influences the chemistry resulting from sulphur ion implantation into solid CO_2 and, by extension, determine whether such chemistry occurring in the Kuiper Belt differs from that arising from analogous implantation processes on Europa. We would like to indicate that a preliminary analysis of our results on the implantation of 290 keV S^+ ions into CO_2 ice at 20 and 70 K was previously published as a letter (Mifsud et al., 2022a); however, in this article, we discuss our results more fully and place a greater emphasis on their applicability to sulphur chemistry in the Kuiper Belt.

Fig. 6 demonstrates that our sulphur ion implantation experiment at 20 K resulted in the appearance of a number of new absorption features in the acquired mid-infrared spectra. Of these features, two weak bands

at 1336 and 1150 cm^{-1} are of particular interest since their positions are in good agreement with those of the asymmetric and symmetric stretching modes of SO_2 , respectively (Schriver-Mazzuoli et al., 2003; Mifsud et al., 2023). It is to be noted, however, that these two absorption bands are fairly weak and are situated in a region of the spectrum where several other, stronger absorption bands are also present. In order to be more confident in our assignment of these bands to SO_2 , we have performed two control experiments. Firstly, the wavenumber peak positions of these bands have been compared with those in an unirradiated $\text{SO}_2:\text{CO}_2$ (1:6) mixed ice prepared by depositing a pre-mixed gas mixture at 20 K (Figs. 6 and 7), and a good agreement (within 1 cm^{-1}) between the positions of the SO_2 asymmetric and symmetric stretching modes in the control spectrum and those suspected to be caused by SO_2 ice in the spectrum of the irradiated ice was found.

Secondly, a control experiment was performed in which a similar fluence of 300 keV He^+ ions was implanted into pure CO_2 ice at 20 K under similar experimental conditions. After the implantation of He^+

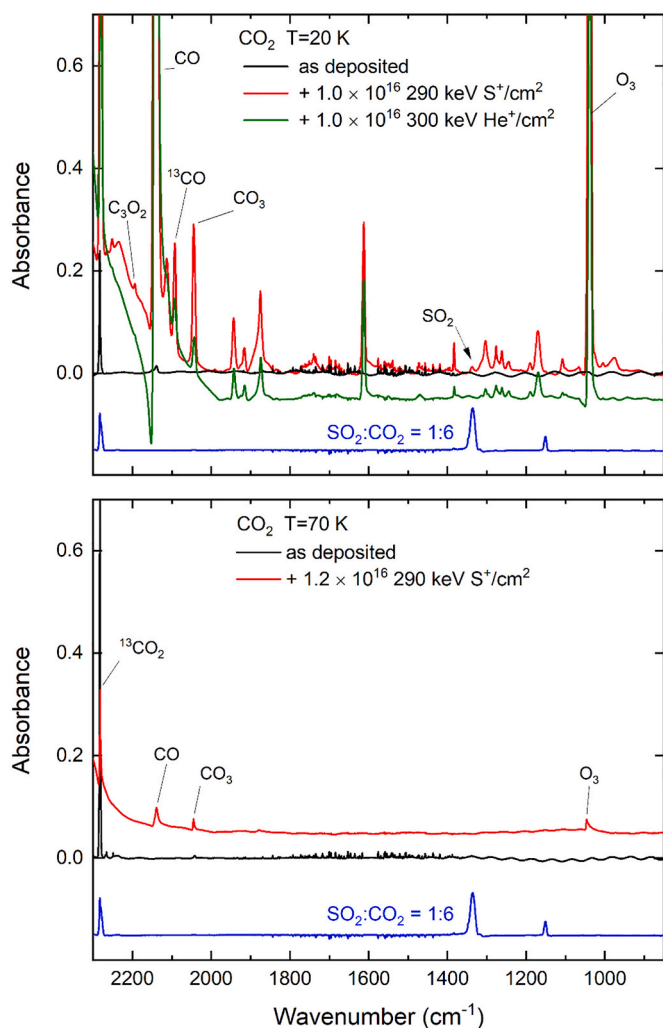


Fig. 6. Mid-infrared spectra of solid CO_2 before (black trace) and after (red trace) the implantation of 290 keV S^+ ions at 20 K (top panel) and 70 K (bottom panel). Also shown are the mid-infrared spectra acquired during control experiments, including an unirradiated $\text{SO}_2:\text{CO}_2$ (1:6) ice mixture at 20 K (blue trace) and a CO_2 ice after the implantation of 300 keV He^+ ions at 20 K (green trace). Note that the spectra of the irradiated ices are difference spectra yielded after the subtraction of the 'as deposited' spectra. Note also that some spectra are vertically shifted for clarity. The data portrayed in this figure are adapted from data initially published in Mifsud et al. (2022a). (For interpretation of the references to colour in this figure legend, the reader is referred to the web version of this article.)

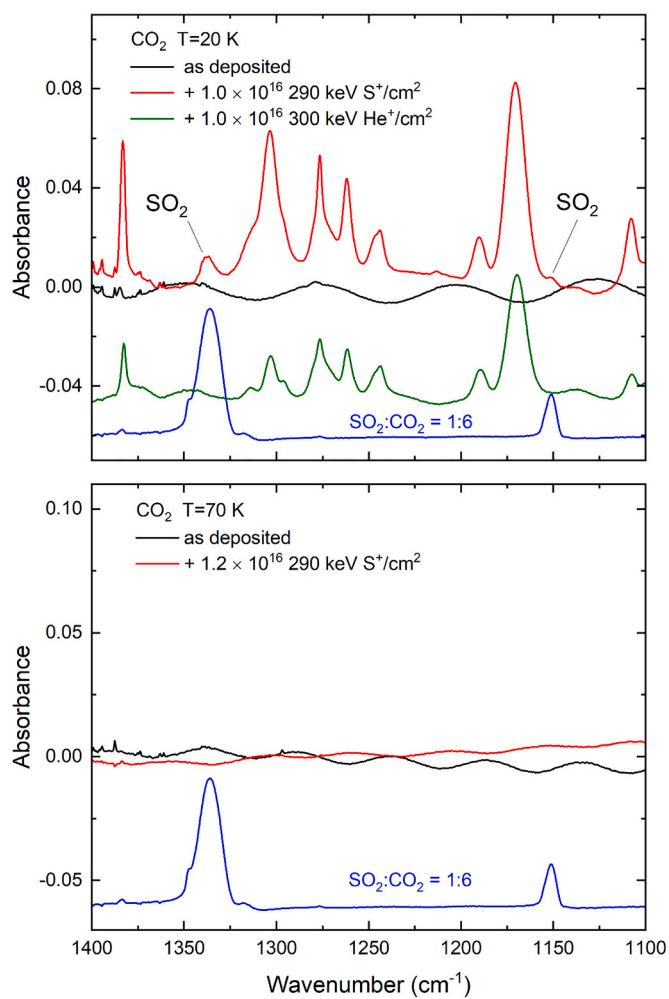


Fig. 7. Mid-infrared spectra of solid CO_2 before (black trace) and after (red trace) the implantation of 290 keV S^+ ions at 20 K (top panel) and 70 K (bottom panel) focusing on the region where the asymmetric and symmetric stretching modes of SO_2 would be expected to appear. Also shown are the mid-infrared spectra of an unirradiated $\text{SO}_2:\text{CO}_2$ (1:6) ice mixture acquired at 20 K (blue trace) and a CO_2 ice after the implantation of 300 keV He^+ ions at 20 K (green trace). Note that the spectra of the irradiated ices are difference spectra yielded after the subtraction of the 'as deposited' spectra. Note also that some spectra are vertically shifted for clarity. The data portrayed in this figure are adapted from data initially published in Mifsud et al. (2022a). (For interpretation of the references to colour in this figure legend, the reader is referred to the web version of this article.)

ions, any mid-infrared absorption bands due to molecules formed as a result of the incorporation of the sulphur ion projectile should be absent, while all other bands produced as a result of the irradiative processing of the ice would still be present. This outcome was indeed observed, and the absorption bands at 1336 and 1150 cm^{-1} were absent throughout the implantation of He^+ ions. Of course, we acknowledge that the implantation of 10^{16} 300 keV He^+ ions cm^{-2} in a CO_2 ice at 20 K results in a different dose administered to the ice than does the implantation of 10^{16} 290 keV S^+ ions cm^{-2} . However, the dose administered as a result of He^+ ion implantation (730 eV per CO_2 molecule) is in fact greater than that administered as a result of S^+ ion implantation (325 eV per CO_2 molecule), and since the absorption bands that were attributed to SO_2 were never observed at any point during He^+ ion implantation, it is reasonable to assume that they are the result of the formation of a molecule that incorporated the sulphur ion projectile.

It is to be noted that other sulphur-bearing molecules, such as SO or S_2O , also present mid-infrared absorption features in the vicinity of 1150 cm^{-1} (Hopkins and Brown, 1975). However, these species are not likely to be the carriers of the bands shown in Figs. 6 and 7 due to their inherent instability. SO, for instance, is a very unstable molecule that has only been isolated in inert matrices at very low temperatures (Hopkins and Brown, 1975). Indeed, the recent work of Góbi et al. (2021) demonstrated that the reaction between hydrogen atoms and SO is favourable at temperatures as low as 3 K. The CO_2 ices considered in this study are certainly not inert matrices due to the energy deposited within the ices during sulphur ion implantation which results in the formation of a plethora of radical species. At 20 K, the temperature is also sufficiently high as to allow for the diffusion of these radicals, thereby ensuring the rapid oxidation of SO to SO_2 (Rolfes et al., 1965; Herron and Huie, 1980; Baklouti et al., 2004). The S_2O molecule is also inherently unstable, and previous literature studies have demonstrated multiple efficient dissociation pathways that would have more than likely dominated within the irradiated CO_2 ices, such as thermal decomposition, dissociative electron attachment, pre-dissociation followed by cleavage of the S—S bond, and disproportionation (Dudley and Hoffmann, 2003; Stuedel and Stuedel, 2004; Field et al., 2005; Navizet et al., 2010).

The chemical reactions leading to the formation of SO_2 proceed after the neutralisation of the implanted sulphur ion. As the neutralised ion traverses the ice, it dissipates energy into its surroundings resulting in the molecular dissociation of CO_2 to CO and an oxygen atom (Pilling et al., 2022; Mifsud et al., 2022c; Mifsud et al., 2022d). The implanted sulphur atom may then react with one such oxygen atom to directly yield SO (Tevault and Smardzewski, 1978). Alternatively, SO may be yielded as a result of the abstraction of an oxygen atom from a surviving CO_2 molecule by the sulphur atom (Froese and Goddard, 1993). SO is then rapidly oxidised to SO_2 , as discussed above. Unfortunately, due to the very small areas of the SO_2 absorption bands in our acquired spectra (Figs. 6 and 7), it has not been possible to accurately determine the evolution of the SO_2 column density as a function of fluence and, from thence, the SO_2 formation efficiency as was done for the study of sulphur ion implantation into solid O_2 .

In contrast, no SO_2 was detected as a result of the implantation of 290 keV S^+ ions into CO_2 ice at 70 K (Figs. 6 and 7). Indeed, the mid-infrared spectrum of the CO_2 ice into which S^+ ions had been implanted at this temperature shows significantly fewer absorption features than does its 20 K counterpart. One particularly notable difference is the intensity of the band related to the O_3 asymmetric stretching mode at approximately 1041 cm^{-1} (Chaabouni et al., 2000). In the 20 K spectrum, this band is very intense and is indicative of a productive chemistry leading to the formation of O_3 during the irradiation of the CO_2 ice. In the 70 K spectrum, however, this band is significantly weaker, which suggests that the irradiative formation of O_3 is much less favourable at this temperature. It is this observation that gives us some insight into why the formation of SO_2 as a result of the implantation of reactive sulphur ions into solid CO_2 is favourable at 20 K, but not at 70 K.

The irradiation of CO_2 ice by ions, electrons, and ultraviolet photons is known to yield several oxygen-bearing products, among which is O_3 (Sivaraman et al., 2013; Martín-Doménech et al., 2015; Mifsud et al., 2022c; Mifsud et al., 2022d). The formation of O_3 is, however, dependent upon the prior formation of O_2 within the ice which is subsequently able to participate in an energetically barrierless reaction with a suprathermal oxygen atom (Sivaraman et al., 2007). In the 20 K ion implantation experiment, nascent O_2 is stable within the ice as the experimental temperature is lower than its sublimation temperature (Collings et al., 2003; Fray and Schmitt, 2009), and so O_3 synthesis may proceed. Indeed, O_3 is a major product of this sulphur ion implantation process (Fig. 6). At 70 K, however, the out-gassing of nascent O_2 from the irradiated ice is known to be fairly efficient (Vidal et al., 1997; Baragiola and Bahr, 1998; Jones et al., 2014), and so the ice is progressively depleted of its oxygen content during irradiation. The net result of this depletion is that there are fewer oxygen atoms available within the bulk ice that may react with the implanted and neutralised sulphur ion to form SO_2 . This therefore explains the non-detection of SO_2 as well as the relative paucity of O_3 in our 70 K experiment.

Prior studies have suggested that otherwise volatile solid-phase molecules such as O_2 may in fact be stabilised at temperatures beyond their sublimation point via their encapsulation within clathrate-like structures. It is possible to speculate that, in our experiments, such CO_2 -based clathrate-like structures may not have been sufficiently stable as to retain O_2 to any meaningful extent at 70 K due to the fact that CO_2 itself is also a fairly volatile species. This interpretation is perhaps even more interesting in light of the previous results of Teolis et al. (2006) who clearly demonstrated that, when making use of a simultaneous deposition-irradiation methodology during ion irradiation experiments, there is an enhancement of the trapping of volatiles (such as O_2) caused by the deposition of fresh overlayers of ice. This trapping was found to be dependent upon the rate of ice deposition used during the simultaneous deposition-irradiation experiment, as well as on the rate of ion delivery (i.e., the ion beam flux) and on the temperature of the irradiation process. For instance, the abundance of radiolytically generated O_2 that was trapped in the ice structure as a result of the simultaneous deposition and irradiation of H_2O ice by 100 keV Ar^+ ions was found to increase as experimental temperatures were raised from 60 to 140 K (Teolis et al., 2006), in line with the increased production of O_2 from irradiated H_2O ice at higher temperatures as reported by Brown et al. (1982).

Parallels may thus be drawn with our present results: the work of Sivaraman et al. (2007) determined that the rate of oxygen atom recombination to yield O_2 increases at higher temperatures, while that of Mifsud et al. (2022c) demonstrated that the production of O_3 as a result of the 1 keV electron irradiation of CO_2 ice increases upon raising the experimental temperature from 20 to 40 K, but subsequently decreases at higher temperatures due to the inefficient trapping of O_2 (the radiolytic precursor to O_3). Both of these works used single deposition or sequential deposition-irradiation methodologies, rather than the simultaneous deposition-irradiation technique used in this study and that of Teolis et al. (2006). Our present results therefore complement and extend these previous findings and provide evidence that the continuous deposition of fresh overlayers of solid CO_2 does not sufficiently preclude O_2 out-gassing as to allow for the efficient formation of oxygen-rich radiolytic products (such as O_3 or SO_2) under the temperature, ion beam flux, and ice deposition conditions considered in our study. Further experimental work should seek to determine whether O_2 may be trapped within irradiated CO_2 ices at 70 K if other combinations of deposition and irradiation conditions are used.

Our work on the implantation of reactive sulphur ions into CO_2 ice has important implications for astrophysics and planetary science. In our previous letter (Mifsud et al., 2022a), we discussed the observed temperature dependence of this physico-chemical process in the context of its applicability (or rather, non-applicability) to the synthesis of the SO_2 observed on the surface of Europa. However, since our results

demonstrate that the synthesis of SO₂ as a result of the implantation of reactive sulphur ions into CO₂ ice is only feasible at temperatures significantly lower than those on the surface of Europa, it is possible that such a mechanism is of greater significance to lower temperature icy KBOs. Indeed, recent data acquired by the *James Webb Space Telescope* have shown that solid CO₂ is a common component of the surface ices of many KBOs (Brown and Fraser, 2023). Given that our results have demonstrated that only a minor and unquantifiable abundance of SO₂ is produced as a result of the implantation of sulphur ions into CO₂ ice at the lowest temperatures that are expected in the Kuiper Belt over a simulated time-scale of 200 million years, and that the efficiency of this synthesis should decrease with increasing temperatures, we are able to further speculate that the implantation of sulphur ions supplied by the solar wind into the surfaces of icy KBOs is likely to account for a very minor fraction of the SO₂ present there. Other sources, such as pre-solar chemical reactions leading to the formation of SO₂ which is then incorporated into the icy KBO during its formation, are likely to be of greater significance.

3.4. On the non-detections of OCS and CS₂

An important observation made during the implantation of sulphur ions into the CO and CO₂ ices considered in this study is the non-detection of either OCS or CS₂ in the irradiated ices. The identification of these species in astronomical environments carries important astrophysical implications due to the known role of these molecules in the catalysis of amino acid oligomerisation to give peptides (Leman et al., 2004; Leman et al., 2015). Moreover, CS₂ is known to partake in oligomerisation and polymerisation processes as a result of its irradiative processing, photo-processing, or its sonochemical treatment (Cataldo, 1995; Cataldo and Heymann, 1998; Heymann et al., 2000; Cataldo, 2000; Cataldo and Heymann, 2001) to yield carbon- and sulphur-rich molecules that may act as a backbone for the production of larger macromolecules with multiple functional groups that may be relevant to biology (Rushdie and Simoneit, 2005). In this present study, no spectroscopic evidence could be found for the formation of OCS or CS₂ after the implantation of sulphur ions into either CO or CO₂ ice at any studied temperature.

In the mid-infrared range, pure OCS presents an absorption band at about 2045 cm⁻¹ which is attributed to the asymmetric stretching of its C=O bond; however, this band is known to experience large shifts in its position of up to 30 cm⁻¹ when OCS is a component of a mixed ice (Ferrante et al., 2008; Garozzo et al., 2010; Sivaraman, 2016). Indeed, an absorption band at the approximately correct position was observed in the CO and CO₂ ices into which sulphur ions were implanted at 20 K (Figs. 4 and 6); however, this band was attributed to CO₃, which also presents an absorption feature in this region of the mid-infrared spectrum. Identifying whether the band at approximately 2045 cm⁻¹ is caused by the presence of OCS or CO₃ may be achieved through an analysis of its full-width at half-maximum (FWHM). OCS presents a broad absorption feature whose FWHM varies between 15 and 20 cm⁻¹ depending on the composition of the ice (Ferrante et al., 2008). Conversely, the FWHM for the CO₃ band is significantly smaller at 5–8 cm⁻¹ (Ferrante et al., 2008; Lv et al., 2014). Given that the bands observed in Figs. 4 and 6 did not have a FWHM that exceeded 7 cm⁻¹, these bands were attributed to the presence of CO₃. Moreover, it should be noted that the bands attributed to CO₃ in the present experiments were weak in the case of the ion-implanted CO ice but intense in the case of the ion-implanted CO₂, which agrees well with the literature data on the abundance of CO₃ formed after the irradiation of CO and CO₂ (Satorre et al., 2000; Trotter and Brooks, 2004; Jamieson et al., 2006; Bennett et al., 2010; Sivaraman et al., 2013; Mifsud et al., 2022c; Mifsud et al., 2022d). Conversely, such an observation contradicts reported trends of OCS formation after the implantation of sulphur ions into these ices, which has been observed after ion implantation into CO ice but not CO₂ ice.

Previous studies by Lv et al. (2014) noted the formation of OCS after the implantation of 176 keV S¹¹⁺ ions into CO ice at 15 K; however, it must be noted that only a very small amount of this radiolytic product was synthesised. Indeed, the absorbance band attributed to OCS was too small for its column density to be quantified even after a fluence of 3.7 × 10¹⁶ sulphur ions cm⁻² had been delivered. This suggests that the formation of OCS as a result of sulphur ion implantation into a carbon oxide ice may not be an efficient chemical process, possibly due to the propensity of OCS to undergo rapid molecular dissociation under the influence of ionising radiation (Ferrante et al., 2008). Given that the abundance of OCS formed in the experiments of Lv et al. (2014) was below their limit of quantitation, it is perhaps unsurprising that we have not been able to find evidence for the formation of OCS in our experiments, which made use of lower implanted sulphur ion fluences.

With regards to CS₂, although a number of previous studies have considered the radiation chemistry of this molecule either as a pure ice or mixed with other molecules in an astrophysical ice analogue (Cataldo, 2000; Maity and Kaiser, 2013; Sivaraman, 2016), less attention has been paid to its radiolytic synthesis from other carbon- and sulphur-bearing precursor species. To the best of our knowledge, only the study of Lv et al. (2014) has identified the formation of CS₂ as a result of the implantation of sulphur ions into a carbon-rich ice. In that study, the presence of CS₂ as a result of the implantation of 90 keV S⁹⁺ ions into CO₂ ice at 15 K was confirmed by the appearance of a small band at about 1510 cm⁻¹, and an upper limit to its formation efficiency of 0.027 molecules per impinging ion was quantified. Given the paucity of experimental work that has sought to understand the formation chemistry of CS₂ under astrophysical conditions, we can only speculate that the formation efficiency quantified by Lv et al. (2014) is also applicable to our study; in which case the maximum column density expected as a result of the implantation of 290 keV S⁺ ions into CO₂ ice at 20 K in our experiments is on the order of 2.7 × 10¹⁴ CS₂ molecules cm⁻², which is below the limit of quantitation of our spectroscopic instrumentation.

4. Conclusions

In this paper, we have discussed the results obtained from a series of systematic sulphur ion implantation experiments into a number of oxygen-bearing ices under conditions that are analogous to those in the Kuiper Belt. In particular, we have implanted a fluence of circa 10¹⁶ S⁺ ions cm⁻² into O₂ ice at 20 K, CO ice at 20 K, and CO₂ ice at both 20 and 70 K. The primary motivation behind our work was to determine whether or not such implantation processes could lead to the formation of simple inorganic sulphurous molecules (such as SO₂, OCS, or CS₂) and, if so, whether such a process could contribute to the sulphur chemistry occurring on the surfaces of icy KBOs.

Our work on the implantation of sulphur ions into solid O₂ has revealed that SO₂ is formed at a rate of 0.47 (±0.01) SO₂ molecules per impinging 400 keV S⁺ ion. Our work constitutes the first study of this processes using mid-infrared absorption spectroscopy as the analytical technique used to identify radiolytic product molecules, and therefore complements and extends previous work performed in the ultraviolet spectral range. The implantation of solar wind sulphur ions may thus represent a non-negligible route towards the synthesis of SO₂ in, for example, cometary ices; although it should be noted that this formation mechanism likely occurs in competition with other radiation and thermal processes in such astrophysical ices, which could therefore decrease the net abundance of SO₂ formed.

No sulphurous molecules could be unambiguously identified after the implantation of sulphur ions into CO ice at 20 K, although some tentative evidence for the formation of SO₂ was presented. Rather, the formation of cumulene dioxides and oxocarbon radicals, together with CO₂ and CO₃, dominated the radiation chemistry occurring within the ice. The apparent inefficiency of SO₂ formation as a result of the implantation of sulphur ions into CO ice raises some questions as to the final form of the implanted sulphur ions. Based on previous work by Ruf

et al. (2019) and Ruf et al. (2021), it is possible to speculate that organosulphur molecules or sulphur-containing residues may have been produced in abundances too low to have been detected by mid-infrared absorption spectroscopy.

Finally, our sulphur ion implantations into CO₂ ice demonstrated that SO₂ could indeed be formed as a radiolytic product at 20 K, but that this synthesis is temperature-dependent and does not occur at a higher temperature of 70 K. This suggests that the chemistry arising from the implantation of sulphur ions into CO₂-rich icy KBOs at low temperatures may differ from that arising from analogous sulphur ion implantations into higher-temperature icy bodies containing solid CO₂, such as Europa. It is anticipated that these results will provide a strong motivation for future experiments seeking to better comprehend the physical and chemical outcomes of sulphur ion implantations into astrophysical ice analogues at various temperatures and using even higher projectile ion fluences.

Declaration of Competing Interest

The authors hereby formally declare that this research was performed in the absence of commercial or financial relationships which may be construed as a conflict of interest.

Data availability

Data will be made available to interested parties upon reasonable request of one of the corresponding authors.

Appendix A. Previous experimental sulphur ion implantation studies

The following table (Table 4) provides a summary of the previous experimental studies that have considered the implantation of reactive sulphur ions into astrophysical ice analogues. More details on the results of these studies may be found in the individual works, as well as in the review article by Mifsud et al. (2021a).

Table 4
Summary of previous experimental studies on the implantation of reactive sulphur ions into ices.

#	Reference	Sulphur Projectile	Target Ice	Temperature (K)
1	Strazzulla et al. (2007)	200 keV S ⁺	H ₂ O	80 K
2a	Ding et al. (2013)	35 keV S ⁷⁺	H ₂ O	80 K
2b	Ding et al. (2013)	90 keV S ⁹⁺	H ₂ O	80 K
2c	Ding et al. (2013)	105 keV S ⁷⁺	H ₂ O	80 K
2d	Ding et al. (2013)	121 keV S ¹¹⁺	H ₂ O	80 K
2e	Ding et al. (2013)	176 keV S ¹¹⁺	H ₂ O	80 K
3a	Lv et al. (2014)	176 keV S ¹¹⁺	CO	15 K
3b	Lv et al. (2014)	90 keV S ⁹⁺	CO ₂	15 K
4a	Boduch et al. (2016)	144 keV S ⁹⁺	H ₂ O	80 K
4b	Boduch et al. (2016)	144 keV S ⁹⁺	O ₂	16 K
4c	Boduch et al. (2016)	144 keV S ⁹⁺	CO ₂	16 K
4d	Boduch et al. (2016)	144 keV S ⁹⁺	H ₂ O:O ₂ (1:1)	16 K
4e	Boduch et al. (2016)	144 keV S ⁹⁺	H ₂ O:CO ₂ (1:1)	16 K
5	Ruf et al. (2019)	105 keV S ⁷⁺	H ₂ O:CH ₃ OH:NH ₃ (2:1:1)	10 K
6	Ruf et al. (2021)	105 keV S ⁷⁺	Organic residues	10 K
7a	Mifsud et al. (2022a)	290 keV S ⁺	CO ₂	20 K
7b	Mifsud et al. (2022a)	290 keV S ⁺	CO ₂	70 K

References

Ahrens, C., Meraviglia, H., Bennett, C., 2022. A geoscientific review on CO and CO₂ ices in the outer solar system. *Geosci.* 12, 51.
 Altwegg, K., 2018. Chemical highlights from the Rosetta Mission. *Proc. Int. Astron. Union* 13, 153.
 Anders, C., Urbassek, H.M., 2019a. High-energy ion impacts into the Sulphur-bearing ice surface of Europa: an atomistic study of chemical transformations. *Astron. Astrophys.* 625, 140.
 Anders, C., Urbassek, H.M., 2019b. Energetic Sulphur ion impacts into cometary ice surfaces: a molecular dynamics study. *Mon. Not. R. Astron. Soc.* 482, 2374.

Acknowledgements

The authors acknowledge support from the Europlanet 2024 RI which has been funded by the European Union's Horizon 2020 Research Innovation Programme under grant agreement No. 871149. The main components of the ICA set-up were purchased using funds obtained from the Royal Society through grants UF130409, RGF/EA/180306, and URF/R/191018. Further developments of the installation were supported in part by the Eötvös Loránd Research Network through grants ELKH IF-2/2019 and ELKH IF-5/2020. This work has also received support from the European Union and the State of Hungary; co-financed by the European Regional Development Fund through grant GINOP-2.3.3-15-2016-00005. Support has also been received from the Research, Development, and Innovation Fund of Hungary through grant K128621. This paper is also based on work from the COST Action CA20129 MultiChem, supported by COST (European Cooperation in Science and Technology). DVM is the recipient of a University of Kent Vice-Chancellor's Research Scholarship. The research of ZK is supported by the Slovak Grant Agency for Science (grant 2/0059/22) and the Slovak Research and Development Agency (contract No. APVV-19-0072). ZJ is grateful for the support of the Hungarian Academy of Sciences through the János Bolyai Research Scholarship. SI acknowledges support from the Danish National Research Foundation through the Centre of Excellence 'InterCat' (grant agreement No. DNR150) and from the Royal Society.

Ashkenazy, Y., 2019. The Surface Temperature of Europa. *Heliyon* 5, e01908.
 Baklouti, D., Schmitt, B., Brissaud, O., 2004. Infrared study of lower Sulphur oxides on Io's surface. *Bull. Am. Astron. Soc.* 36 (16), 07.
 Bang, J., Shoaib, M.A., Choi, C.H., Kang, H., 2017. Efficient thermal reactions of Sulphur dioxide on ice surfaces at low temperature: a combined experimental and theoretical study. *ACS Earth Space Chem.* 1, 503.
 Baragiola, R.A., 2003. Water ice on outer solar system surfaces: basic properties and radiation effects. *Planet. Space Sci.* 51, 953.
 Baragiola, R.A., Bahr, D.A., 1998. Laboratory studies of the optical properties and stability of oxygen on Ganymede. *J. Geophys. Res. Planet.* 103, 25865.

- Becker, T.M., Trumbo, S.K., Molyneux, P.M., Retherford, K.D., Hendrix, A.R., Roth, L., Raut, U., Alday, J., McGrath, M.A., 2022. Mid-ultraviolet *Hubble* observations of Europa and the global surface distribution of SO₂. *Planet. Sci. J.* 3, 129.
- Bennett, C.J., Kaiser, R.I., 2005. Laboratory studies on the formation of ozone (O₃) on icy satellites and on interstellar and cometary ices. *Astrophys. J.* 635, 1362.
- Bennett, C.J., Jamieson, C.S., Kaiser, R.I., 2010. Mechanical studies on the formation and destruction of carbon monoxide (CO), carbon dioxide (CO₂), and carbon trioxide (CO₃) in interstellar ice analogue samples. *Phys. Chem. Chem. Phys.* 12, 4032.
- Bieler, A., Altwegg, K., Balsiger, H., Bar-Nun, A., Berthelier, J.-J., Bochsler, P., Briosis, C., Calmonte, U., Combi, M., De Keyser, J., van Dishoeck, E.F., Fiethe, B., Fuselier, S.A., Gasc, S., Gombosi, T.I., Hansen, K.C., Hässig, M., Jäckel, A., Kopp, E., Korth, A., Le Roy, L., Mall, U., Maggioni, R., Marty, B., Mousis, O., Owen, T., Rème, H., Rubin, M., Sémon, T., Tzou, C.-Y., Waite, J.H., Walsh, C., Wurz, P., 2015. Abundant molecular oxygen in the coma of comet 67P/Churyumov-Gerasimenko. *Nature* 526, 678.
- Biri, S., Vajda, I., Hajdu, P., Rácz, R., Csík, A., Kormány, Z., Perduk, Z., Kocsis, F., Rajta, I., 2021. The Atomki accelerator Centre. *Eur. Phys. J. Plus* 136, 247.
- Boduch, P., Brunetto, R., Ding, J.J., Domaracka, A., Kaňuchová, Z., Palumbo, M.E., Rothard, H., Strazzulla, G., 2016. Ion processing of ices and the origin of SO₂ and O₃ on the icy surfaces of the icy Jovian satellites. *Icarus* 277, 424.
- Brown, M.E., Fraser, W.C., 2023. The state of CO and CO₂ ices in the Kuiper Belt as seen by JWST. *Planet. Sci. J.* 4, 130.
- Brown, W.L., Augustyniak, W.M., Simmons, E., Marcantonio, K.J., Lanzerotti, L.J., Johnson, R.E., Boring, J.W., Reimann, C.T., Foti, G., Pirronello, V., 1982. Erosion and molecule formation in condensed gas films by electronic energy loss of fast ions. *Nucl. Inst. Methods Phys. Res. A* 198, 1.
- Calmonte, U., Altwegg, K., Balsiger, H., Berthelier, J.J., Bieler, A., Cessateur, G., Dhoooghe, F., van Dishoeck, E.F., Fiethe, B., Fuselier, S.A., Gasc, S., Gombosi, T.I., Hässig, M., Le Roy, L., Rubin, M., Sémon, T., Tzou, C.-Y., Wampfler, S.F., 2016. Sulphur-bearing species in the coma of comet 67P/Churyumov-Gerasimenko. *Mon. Not. R. Astron. Soc.* 462, S253.
- Carlson, R.W., Johnson, R.E., Anderson, M.E., 1999. Sulphur acid on Europa and the Radiolytic Sulphur cycle. *Science* 286, 97.
- Carlson, R.W., Anderson, M.S., Johnson, R.E., Schulman, M.B., Yavrouian, A.H., 2002. Sulphuric acid production on Europa: the radiolysis of Sulphur in water ice. *Icarus* 157, 456.
- Cataldo, F., 1995. On the Photopolymerisation of carbon Disulphide. *Inorg. Chim. Acta* 232, 27.
- Cataldo, F., 2000. On the Radiopolymerisation of carbon Disulphide. *Radiat. Phys. Chem.* 58, 217.
- Cataldo, F., Heymann, D., 1998. Carbon Disulphide Sonopolymer: a comparison with other carbon Disulphide polymers. *Eur. J. Solid State Inorg. Chem.* 35, 619.
- Cataldo, F., Heymann, D., 2001. Comparison of the soluble products from radiolysis and photolysis of CS₂. *Radiat. Phys. Chem.* 61, 115.
- Chaabouni, H., Schriver-Mazzuoli, L., Schriver, A., 2000. Infrared spectroscopy of neat solid ozone and that of ozone in interaction with amorphous and crystalline water ice. *J. Phys. Chem. A* 104, 6962.
- Collings, M.P., Anderson, M.A., Chen, R., Dever, J.W., Viti, S., Williams, D.A., McCoustra, M.R.S., 2003. A laboratory survey of the thermal desorption of Astrophysically relevant molecules. *Mon. Not. R. Astron. Soc.* 354, 1133.
- Cruikshank, D.P., Grundy, W.M., DeMeo, F.E., Buie, M.W., Binzel, R.P., Jennings, D.E., Olkin, C.B., Parker, J.W., Reuter, D.C., Spencer, J.R., Stern, S.A., Young, L.A., Weaver, H.A., 2015. The surface compositions of Pluto and Charon. *Icarus* 246, 82.
- Dalton, J.B., Cassidy, T., Paranicas, C., Shirley, J.H., Prockter, L.M., Kamp, L.W., 2013. Exogenic controls on Sulphuric acid hydrate production at the surface of Europa. *Planet. Space Sci.* 77, 45.
- de Barros, A.L.F., Seperuelo Duarte, E., Farenzena, L.S., da Silveira, E.F., Domaracka, A., Rothard, H., Boduch, P., 2011. Destruction of CO ice and formation of new molecules by irradiation with 28 keV O⁶⁺ ions. *Nucl. Instrum. Methods Phys. Res. B: Beam Interactions Mater. Atom.* 269, 852.
- Ding, J.J., Boduch, P., Domaracka, A., Guillois, S., Langlinay, T., Lv, X.Y., Palumbo, M. E., Rothard, H., Strazzulla, G., 2013. Implantation of multiply charged Sulphur ions in water ice. *Icarus* 226, 860.
- Dogliotti, L., Hayon, E., 1968. Flash photolysis study of Sulphite, thiocyanate, and Thiosulphate ions in solution. *J. Phys. Chem.* 72, 1800.
- Dudley, T.J., Hoffmann, M.R., 2003. Theoretical study of the ground and first excited singlet state potential energy surfaces of Disulphur monoxide (S₂O). *Mol. Phys.* 101, 1303.
- Ennis, C.P., Bennett, C.J., Kaiser, R.I., 2011. On the formation of ozone in oxygen-rich solar system ices via Ionising radiation. *Phys. Chem. Chem. Phys.* 13, 9469.
- Erickson, R.E., Yates, L.M., Clark, R.L., McEwen, D., 1977. The reaction of Sulphur dioxide with ozone in water and its possible atmospheric significance. *Atmos. Environ.* 11, 813.
- Famá, M., Bahr, D.A., Teolis, B.D., Baragiola, R.A., 2002. Ion beam induced chemistry: the case of ozone synthesis and its influence on the sputtering of solid oxygen. *Nucl. Instrum. Methods Phys. Res. B: Beam Interactions Mater. Atom.* 193, 775.
- Ferrante, R.F., Moore, M.H., Spiliotis, M.M., Hudson, R.L., 2008. Formation of interstellar OCS: radiation chemistry and IR spectra of precursor ices. *Astrophys. J.* 684, 1210.
- Field, T.A., Slattery, A.E., Adams, D.J., Morrison, D.D., 2005. Experimental observation of dissociative Electron attachment to S₂O and S₂O₂ with a new spectrometer for unstable molecules. *J. Phys. B: Atom. Mol. Opt. Phys.* 38, 255.
- Fray, N., Schmitt, B., 2009. Sublimation of ices of astrophysical interest: a bibliographic review. *Planet. Space Sci.* 57, 2053.
- Freiman, Y.A., Jodl, H.J., 2004. Solid Oxygen. *Phys. Rep.* 401, 1.
- Froese, R.D.J., Goddard, J.D., 1993. *Ab initio* studies of the lowest singlet and triplet potential energy surfaces of CO₂S. *Mol. Phys.* 79, 685.
- Garozzo, M., Fulvio, D., Gomis, O., Palumbo, M.E., Strazzulla, G., 2008. H-implantation in SO₂ and CO₂ ices. *Planet. Space Sci.* 56, 1300.
- Garozzo, M., Fulvio, D., Kaňuchová, Z., Palumbo, M.E., Strazzulla, G., 2010. The fate of S-bearing species after ion irradiation of interstellar icy grain mantles. *Astron. Astrophys.* 509, A67.
- Gerakines, P.A., Moore, M.H., 2001. Carbon suboxide in astrophysical ice analogues. *Icarus* 154, 372.
- Gerakines, P.A., Schutte, W.A., Greenberg, J.M., van Dishoeck, E.F., 1995. The infrared band strengths of H₂O, CO, and CO₂ in laboratory simulations of astrophysical ice mixtures. *Astron. Astrophys.* 296, 810.
- Giammanco, C., Bochsler, P., Karrer, R., Ipavich, F.M., Paquette, J.A., Wurz, P., 2007. Determination of Sulphur abundance in the solar wind. *Space Sci. Rev.* 130, 329.
- Góbi, S., Csonka, I.P., Bazsó, G., Tarczay, Gy., 2021. Successive hydrogenation of SO and SO₂ in solid *Para*-H₂: formation of elusive small oxoacids of Sulphur. *ACS Earth Space Chem.* 5, 1180.
- Grieves, G.A., Orlando, T.M., 2005. The importance of pores in the Electron stimulated production of D₂ and O₂ in low temperature ice. *Surf. Sci.* 593, 180.
- Grundy, W.M., Young, L.A., Stansberry, L.A., Buie, M.W., Olkin, C.B., Young, E.F., 2010. Near-infrared spectral monitoring of Triton with IRTF/SpeX II: spatial distribution and evolution of ices. *Icarus* 205, 594.
- Grundy, W.M., Binzel, R.P., Buratti, B.J., Cook, J.C., Cruikshank, D.P., Dalle Ore, C.M., Earle, A.M., Ennico, K., Howett, C.J.A., Lunsford, A.W., Olkin, C.B., Parker, A.H., Philippe, S., Protopata, S., Quirico, E., Reuter, D.C., Schmitt, B., Singer, K.N., Verbiscer, A.J., Beyer, R.A., Buie, M.W., Cheng, A.F., Jennings, D.E., Linscott, I.R., Parker, J.W.M., Schenk, P.M., Spencer, J.R., Stansberry, J.A., Stern, S.A., Throop, H. B., Tsang, C.C.C., Weaver, H.A., Weigle, G.E., Young, L.A., the New Horizons Science Team, 2016. Surface compositions across Pluto and Charon. *Science* 351, 1283.
- Hallbrucker, A., Mayer, E., 1990. Unexpectedly stable nitrogen, oxygen, carbon monoxide, and argon clathrate hydrates from vapour-deposited amorphous solid water: an X-ray and two-step differential scanning calorimetry study. *J. Chem. Soc. Faraday Trans.* 86, 3785.
- Hand, K.P., Carlson, R.W., Chyba, C.F., 2007. Energy, chemical disequilibrium, and geological constraints on Europa. *Astrobiology* 7, 1006.
- Hansen, G.B., McCord, T.B., 2008. Widespread CO₂ and other non-ice compounds on the anti-Jovian and trailing sides of Europa from *Galileo*/NIMS observations. *Geophys. Res. Lett.* 35, L01202.
- Hendrix, A.R., Cassidy, T.A., Johnson, R.E., Paranicas, C., Carlson, R.W., 2011. Europa's disc-resolved ultraviolet spectra: relationships with plasma flux and surface terrains. *Icarus* 212, 736.
- Herczku, P., Mífsud, D.V., Ioppolo, S., Juhász, Z., Kaňuchová, Z., Kovács, S.T.S., Traspas Muña, A., Hailley, P.A., Rajta, I., Vajda, I., Mason, N.J., McCullough, R.W., Paripás, B., Sulik, B., 2021. The ice chamber for astrophysics-Astrochemistry (ICA): a new experimental Facility for ion Impact Studies of astrophysical ice analogues. *Rev. Sci. Instrum.* 92, 084501.
- Herron, J.T., Huie, R.E., 1980. Rate constants at 298 K for the reactions SO + SO + M → (SO)₂ + M and SO + (SO)₂ → SO₂ + S₂O. *Chem. Phys. Lett.* 76, 322.
- Heymann, D., Cataldo, F., Thieme, M.H., Fokkens, R., Nibbering, N.M.M., Vis, R.D., 2000. Formation of C_mS_n compounds by Photopolymerisation of CS₂ in the atmosphere of Jupiter. *Meteorit. Planet. Sci.* 35, 355.
- Hochanadel, C.J., Ghormley, J.A., Sworski, T.J., 1955. The decomposition of Sulphuric acid by cobalt γ-rays. *J. Am. Chem. Soc.* 77, 3215.
- Holtom, P.D., Dawes, A., Mukerji, R.J., Davis, M.P., Webb, S.M., Hoffmann, S.V., Mason, N.J., 2006. VUV Photoabsorption spectroscopy of Sulphur dioxide ice. *Phys. Chem. Chem. Phys.* 8, 714.
- Hopkins, A.G., Brown, C.W., 1975. Infrared Spectrum of Sulphur monoxide. *J. Chem. Phys.* 62, 2511.
- Ioppolo, S., Cuppen, H.M., Romanzin, C., van Dishoeck, E.F., Linnartz, H., 2008. Laboratory evidence for efficient water formation in interstellar ices. *Astrophys. J.* 686, 1474.
- Isokoski, K., Poteet, C.A., Linnartz, H., 2013. Highly resolved infrared spectra of pure CO₂ ice (15–75 K). *Astron. Astrophys.* 555, A85.
- Jamieson, C.S., Mebel, A.M., Kaiser, R.I., 2006. Identification of the *D*_{3h} isomer of carbon trioxide (CO₃) and its Implications for atmospheric chemistry. *Chem. Phys. Chem.* 7, 2508.
- Jones, B.M., Kaiser, R.I., Strazzulla, G., 2014. UV-Vis, infrared, and mass spectroscopy of Electron irradiated frozen oxygen and carbon dioxide mixtures with water. *Astrophys. J.* 781, 85.
- Kaňuchová, Z., Boduch, P., Domaracka, A., Palumbo, M.E., Rothard, H., Strazzulla, G., 2017. Thermal and energetic processing of astrophysical ice analogues rich in SO₂. *Astron. Astrophys.* 604, A68.
- Kossacki, K.J., Szutowicz, S., 2010. Comet 17P/Holmes: possibility of a CO driven explosion. *Icarus* 212, 847.
- Kossacki, K.J., Szutowicz, S., 2013. Activity of comet 29P/Schwassmann-Wachmann 1. *Icarus* 225, 111.
- Lee, J.H., Michael, J.V., Payne, W.A., Stief, L.J., 1978. Absolute rate of the reaction of hydrogen atoms with ozone from 219–360 K. *J. Chem. Phys.* 69, 350.
- Leman, L., Orgel, L., Ghadiri, M.R., 2004. Carbonyl Sulphide-mediated prebiotic formation of peptides. *Science* 306, 283.
- Leman, L., Huang, Z.-Z., Ghadiri, M.R., 2015. Peptide bond formation in water mediated by carbon Disulphide. *Astrobiology* 15, 709.
- Li, J., Li, C., 2023. Sulphur chemistry on the surface ice of Europa. *Icarus* 394, 115438.
- Loeffler, M.J., Hudson, R.L., 2010. Thermally-induced chemistry and the Jovian icy satellites: a laboratory study of the formation of Sulphur oxyanions. *Geophys. Res. Lett.* 37, L19201.
- Loeffler, M.J., Hudson, R.L., 2016. What is eating ozone? Thermal reactions between SO₂ and O₃: implications for icy environments. *Astrophys. J. Lett.* 833, L9.

- Loeffler, M.J., Baratta, G.A., Palumbo, M.E., Strazzulla, G., Baragiola, R.A., 2005. CO₂ synthesis in solid CO by Lyman- α photons and 200 keV protons. *Astron. Astrophys.* 435, 587.
- Loeffler, M.J., Hudson, R.L., Moore, M.H., Carlson, R.W., 2011. Radiolysis of Sulphuric acid, Sulphuric acid monohydrate, and Sulphuric acid Tetrahydrate and its relevance to Europa. *Icarus* 215, 370.
- Luna, R., Millán, C., Domingo, M., Santonja, C., Satorre, M.Á., 2022. Density and refractive index of carbon monoxide ice at different temperatures. *Astrophys. J.* 935, 134.
- Luspay-Kuti, A., Mousis, O., Lunine, J.I., Ellinger, Y., Pauzat, F., Raut, U., Bouquet, A., Mandt, K.E., Maggilo, R., Ronnet, T., Brugger, B., Ozgurel, O., Fuselier, S.A., 2018. Origin of molecular oxygen in comets: current knowledge and perspectives. *Space Sci. Rev.* 214, 115.
- Lv, X.Y., Boduch, P., Ding, J.J., Domaracka, A., Langlinay, T., Palumbo, M.E., Rothard, H., Strazzulla, G., 2014. Sulphur implantation in CO and CO₂ ices. *Mon. Not. R. Astron. Soc.* 438, 922.
- Mahjoub, A., Altwegg, K., Poston, M.J., Rubin, M., Hodyss, R., Choukroun, M., Ehlmann, B.L., Hänni, N., Brown, M.E., Blacksborg, J., Eiler, J.M., Hand, K.P., 2023. Complex Organosulphur molecules on comet 67P: evidence from the ROSINA measurements and insights from laboratory simulations. *Sci. Adv.* 9, eadh0394.
- Maity, S., Kaiser, R.I., 2013. Electron irradiation of carbon Disulphide-oxygen ices: toward the formation of Sulphur-bearing molecules in interstellar ices. *Astrophys. J.* 773, 184.
- Martín-Doménech, R., Manzano-Santamaría, J., Muñoz-Caro, G.M., Cruz-Díaz, G.A., Chen, Y.-J., Herrero, V.J., Tanarro, I., 2015. UV Photoprocessing of CO₂ ice: a complete quantification of photochemistry and photon-induced desorption processes. *Astron. Astrophys.* 584, 14.
- Mason, N.J., Dawes, A., Holtom, P.D., Mukerji, R.J., Davis, M.P., Sivaraman, B., Kaiser, R.I., Hoffmann, S.V., Shaw, D.A., 2006. VUV spectroscopy and photoprocessing of astrochemical ices: an experimental study. *Faraday Discuss.* 133, 311.
- Mayer, E., Hallbrucker, A., 1989. Unexpectedly stable nitrogen and oxygen clathrate hydrates from vapour deposited amorphous solid water. *J. Chem. Soc. Chem. Commun.* 1989, 749.
- McCORD, T.B., Hansen, G.B., Clark, R.N., Martin, P.D., Hibbitts, C.A., Fanale, F.P., Granahan, J.C., Segura, M., Matson, D.L., Johnson, T.V., Carlson, R.W., Smythe, W. D., Danielson, G.E., 1998. Non-water-ice constituents in the surface material of the icy Galilean satellites from the *Galileo* near-infrared mapping spectrometer investigation. *J. Geophys. Res. Planet.* 103, 8603.
- Mifsud, D.V., Kaňuchová, Z., Herczku, P., Ioppolo, S., Juhász, Z., Kovács, S.T.S., Mason, N.J., McCullough, R.W., Sulik, B., 2021a. Sulphur ice Astrochemistry: a review of laboratory studies. *Space Sci. Rev.* 217, 14.
- Mifsud, D.V., Juhász, Z., Herczku, P., Kovács, S.T.S., Ioppolo, S., Kaňuchová, Z., Czentye, M., Hailey, P.A., Traspas Muiña, A., Mason, N.J., McCullough, R.W., Paripás, B., Sulik, B., 2021b. Electron irradiation and thermal chemistry studies of interstellar and planetary ice analogues at the ICA Astrochemistry facility. *Eur. Phys. J. D: Atom. Mol. Opt. Plasma Phys.* 75, 182.
- Mifsud, D.V., Kaňuchová, Z., Herczku, P., Juhász, Z., Kovács, S.T.S., Lakatos, G., Rahul, K.K., Rác, R., Sulik, B., Biri, S., Rajta, I., Vajda, I., Ioppolo, S., McCullough, R. W., Mason, N.J., 2022a. Sulphur ion implantations into condensed CO₂: implications for Europa. *Geophys. Res. Lett.* 49, e2022GL100698.
- Mifsud, D.V., Hailey, P.A., Herczku, P., Juhász, Z., Kovács, S.T.S., Sulik, B., Ioppolo, S., Kaňuchová, Z., McCullough, R.W., Paripás, B., Mason, N.J., 2022b. Laboratory experiments on the radiation Astrochemistry of water ice phases. *Eur. Phys. J. D Atom. Mol. Opt. Phys.* 76, 87.
- Mifsud, D.V., Kaňuchová, Z., Ioppolo, S., Herczku, P., Traspas Muiña, A., Field, T.A., Hailey, P.A., Juhász, Z., Kovács, S.T.S., Mason, N.J., McCullough, R.W., Pavithraa, S., Rahul, K.K., Paripás, B., Sulik, B., Chou, S.L., Lo, J.I., Das, A., Cheng, B. M., Rajasekhar, B.N., Bhardwaj, A., Sivaraman, B., 2022c. Mid-IR and VUV spectroscopic characterisation of thermally processed and Electron irradiated CO₂ astrophysical ice analogues. *J. Mol. Spectrosc.* 385, 111599.
- Mifsud, D.V., Kaňuchová, Z., Ioppolo, S., Herczku, P., Traspas Muiña, A., Sulik, B., Rahul, K.K., Kovács, S.T.S., Hailey, P.A., McCullough, R.W., Mason, N.J., Juhász, Z., 2022d. Ozone production in Electron irradiated CO₂:O₂ ices. *Phys. Chem. Chem. Phys.* 24, 10974.
- Mifsud, D.V., Herczku, P., Rahul, K.K., Ramachandran, R., Sundararajan, P., Kovács, S.T. S., Sulik, B., Juhász, Z., Rác, R., Biri, S., Kaňuchová, Z., McCullough, R.W., Sivaraman, B., Ioppolo, S., Mason, N.J., 2023. A systematic mid-infrared spectroscopic study of thermally processed SO₂ ices. *Phys. Chem. Chem. Phys.* 25, 26278.
- Mokrane, H., Chaabouni, H., Accolla, M., Congiu, E., Dulieu, F., Chehrouri, M., Lemaire, J.L., 2009. Experimental evidence for water formation via ozone hydrogenation on dust grains at 10 K. *Astrophys. J.* 705, L195.
- Moore, M.H., Hudson, R.L., Carlson, R.W., 2007. The radiolysis of SO₂ and H₂S in water ice: implications for the icy Jovian satellites. *Icarus* 189, 409.
- Mousis, O., Ronnet, T., Brugger, B., Ozgurel, O., Pauzat, F., Ellinger, Y., Maggilo, R., Wurz, P., Vernazza, P., Lunine, J.I., Luspay-Kuti, A., Mandt, K.E., Altwegg, K., Bieler, A., Markovits, A., Rubin, M., 2016. Origin of molecular oxygen in comet 67P/Churyumov-Gerasimenko. *Astrophys. J. Lett.* 823, L41.
- Navizet, I., Komiha, N., Linguerr, R., Chambaud, G., Rosmus, P., 2010. On the formation of S₂O at low energies: an *ab initio* study. *Chem. Phys. Lett.* 500, 207.
- Palumbo, M.E., Leto, P., Siringo, C., Trigliano, C., 2008. Detection of C₃O in the low-mass Protostar Elias 18. *Astrophys. J.* 685, 1033.
- Penkett, S.A., Jones, B.M.R., Brich, K.A., Eggleton, A.E.J., 1979. The importance of atmospheric ozone and hydrogen peroxide in Oxidising Sulphur dioxide in cloud and rainwater. *Atmos. Environ.* 13, 123.
- Pilling, S., Carvalho, G.A., Rocha, W.R.M., 2022. Chemical evolution of CO₂ ices under processing by Ionising radiation: characterisation of non-observed species and chemical equilibrium phase with the employment of PROCODA code. *Astrophys. J.* 925, 147.
- Rajta, I., Vajda, I., Gyürky, Gy., Csedreki, L., Kiss, Á.Z., Biri, S., van Oosterhout, H.A.P., Podaru, N.C., Mous, D.J.W., 2018. Accelerator characterisation of the new ion beam facility at MTA Atomki in Debrecen, Hungary. *Nucl. Instrum. Methods Phys. Res. A: Acceler. Spectrom. Detect. Assoc. Equip.* 880, 125.
- Rolfes, T.R., Reeves, R.R., Harteck, P., 1965. The chemiluminescent reaction of oxygen atoms with Sulphur monoxide at low pressures. *J. Phys. Chem.* 69, 849.
- Rubin, M., Altwegg, K., van Dishoeck, E.F., Schwehm, G., 2015. Molecular oxygen in Oort cloud comet 1P/Halley. *Astrophys. J. Lett.* 815, L11.
- Rubin, M., Altwegg, K., Balsiger, H., Berthelier, J.-J., Combi, M.R., De Keyser, J., Drozdovskaya, M., Fiethe, B., Fuselier, S.A., Gasc, S., Gombosi, T.I., Hänni, N., Hansen, K.C., Mall, U., Rème, H., Schroeder, I.R.H.G., Schuhmann, M., Sémon, T., Waite, J.H., Wampfler, S.F., Wurz, P., 2019. Elemental and molecular abundances in comet 67P/Churyumov-Gerasimenko. *Mon. Not. R. Astron. Soc.* 489, 594.
- Ruf, A., Bouquet, A., Boduch, P., Schmitt-Kopplin, P., Vinogradoff, V., Duvernay, F., Urso, R.G., Brunetto, R., Le Sergeant d'Hendecourt, L., Mousis, O., Danger, G., 2019. Organosulphur compounds formed by Sulphur ion bombardment of astrophysical ice analogues: implications for moons, comets, and Kuiper Belt objects. *Astrophys. J. Lett.* 885, L40.
- Ruf, A., Bouquet, A., Schmitt-Kopplin, P., Boduch, P., Mousis, O., Danger, G., 2021. Sulphur ion irradiation experiments simulating space weathering of solar system body surfaces. *Astron. Astrophys.* 655, A74.
- Rushdie, A.I., Simoneit, B.R.T., 2005. Abiotic synthesis of organic compounds from carbon Disulphide under hydrothermal conditions. *Astrobiology* 5, 749.
- Satorre, M.Á., Palumbo, M.E., Strazzulla, G., 2000. CO/CO₂ molecular number ratio produced by ion irradiation of ices. *Astrophys. Space Sci.* 274, 643.
- Satorre, M.Á., Domingo, M., Millán, C., Luna, R., Vilaplana, R., Santonja, C., 2008. Density of CH₄, N₂, and CO₂ ices at different temperatures of deposition. *Planet. Space Sci.* 56, 1748.
- Schrivver-Mazzuoli, L., Chaabouni, H., Schriver, A., 2003. Infrared spectra of SO₂ and SO₂:H₂O ices at low temperature. *J. Mol. Struct.* 644, 151.
- Sivaraman, B., 2016. Electron irradiation of carbon dioxide-carbon Disulphide ice analogue and its implication for the identification of carbon Disulphide on the moon. *J. Chem. Sci.* 128, 159.
- Sivaraman, B., Jamieson, C.S., Mason, N.J., Kaiser, R.I., 2007. Temperature-dependent formation of ozone in solid oxygen by 5 keV Electron irradiation and implications for solar system ices. *Astrophys. J.* 669, 1414.
- Sivaraman, B., Rajasekhar, B.N., Fulvio, D., Hunniford, A., McCullough, R.W., Palumbo, M.E., Mason, N.J., 2013. Ozone and carbon trioxide synthesis by low energy ion implantation onto solid carbon dioxide and implications to Astrochemistry. *J. Chem. Phys.* 139, 074706.
- Smith, L.R., Gudipati, M.S., Smith, R.L., Lewis, R.D., 2021. Isotope effect on the sublimation curves and binding energies of ¹²CO and ¹³CO interstellar ice analogues. *Astron. Astrophys.* 656, A82.
- Stuedel, R., Stuedel, Y., 2004. The thermal decomposition of S₂O forming SO₂, S₃, S₄, and S₅O: an *ab initio* MO study. *Eur. J. Inorg. Chem.* 2004, 3513.
- Strazzulla, G., Brucato, J.R., Palumbo, M.E., Satorre, M.Á., 1997. Is it possible to detect frozen O₂ and N₂ on interstellar grains? *Astron. Astrophys.* 321, 618.
- Strazzulla, G., Baratta, G.A., Leto, G., Gomis, O., 2007. Hydrate Sulphuric acid after Sulphur implantation in water ice. *Icarus* 192, 623.
- Strazzulla, G., Garozzo, M., Gomis, O., 2009. The origin of Sulphur-bearing species on the surfaces of icy satellites. *Adv. Space Res.* 43, 1442.
- Teolis, B.D., Vidal, R.A., Shi, J., Baragiola, R.A., 2005. Mechanisms of O₂ sputtering from water ice by keV ions. *Phys. Rev. B* 72, 245422.
- Teolis, B.D., Loeffler, M.J., Raut, U., Famá, M., Baragiola, R.A., 2006. Ozone synthesis on the icy satellites. *Astrophys. J.* 644, L141.
- Tevault, D.E., Smardzewski, R.R., 1978. Chemiluminescent reactions of Sulphur atoms and oxygen atoms in solid argon matrices. SO Chemiluminescence. *J. Chem. Phys.* 69, 3182.
- Trottier, A., Brooks, R.L., 2004. Carbon-chain oxides in proton-irradiated CO ice films. *Astrophys. J.* 612, 1214.
- Vidal, R.A., Bahr, D., Baragiola, R.A., Peters, M., 1997. Oxygen on Ganymede: laboratory Science 276, 1839.
- von Steiger, R., Zurbuchen, T.H., McComas, D.J., 2010. Oxygen flux in the solar wind: Ulysses observations. *Geophys. Res. Lett.* 37, L22101.
- Waygood, S.J., McElroy, W.J., 1992. Spectroscopy and decay kinetics of the Sulphite radical anion in aqueous solution. *J. Chem. Soc. Faraday Trans.* 88, 1525.
- Zheng, W., Jewitt, D., Kaiser, R.I., 2006a. Formation of hydrogen, oxygen, and hydrogen peroxide in Electron-irradiated crystalline water ice. *Astrophys. J.* 639, 534.
- Zheng, W., Jewitt, D., Kaiser, R.I., 2006b. Temperature dependence of the formation of hydrogen, oxygen, and hydrogen peroxide in Electron-irradiated crystalline water ice. *Astrophys. J.* 648, 753.
- Zheng, W., Jewitt, D., Kaiser, R.I., 2007. Electron irradiation of crystalline and amorphous D₂O ice. *Chem. Phys. Lett.* 435, 289.
- Ziegler, J.F., Ziegler, M.D., Biersack, J.P., 2010. SRIM – The Stopping and Range of Ions in Matter (2010). *Nucl. Instrum. Meth. Phys. Res. B: Beam Interact. Mater. Atom.* 268, 1818.